

University of Mississippi

eGrove

Faculty and Student Publications

Biology

1-1-2019

Analysis of *Brevundimonas subvibrioides* developmental signaling systems reveals inconsistencies between phenotypes and c-di-GMP levels

Lauryn Sperling

University of Mississippi

Milagros D. Mulero Alegría

University of Mississippi

Volkhard Kaever

Medizinische Hochschule Hannover (MHH)

Patrick D. Curtis

University of Mississippi

Follow this and additional works at: https://egrove.olemiss.edu/biology_facpubs

Recommended Citation

Sperling, L., Mulero Alegría, M. D., Kaever, V., & Curtis, P. D. (2019). Analysis of *Brevundimonas subvibrioides* Developmental Signaling Systems Reveals Inconsistencies between Phenotypes and c-di-GMP Levels. *Journal of Bacteriology*, 201(20), e00447-19, /jb/201/20/JB.00447-19.atom. <https://doi.org/10.1128/JB.00447-19>

This Article is brought to you for free and open access by the Biology at eGrove. It has been accepted for inclusion in Faculty and Student Publications by an authorized administrator of eGrove. For more information, please contact egrove@olemiss.edu.

1 **Analysis of *Brevundimonas subvibrioides* developmental signaling systems reveals**
2 **inconsistencies between phenotypes and c-di-GMP levels**

3

4 Running title: *Brevundimonas* developmental signaling and c-di-GMP

5 Keywords: *Brevundimonas*, *Caulobacter*, development, signaling, DivK, c-di-GMP

6

7 Lauryn Sperling¹, Milagros D. Mulero Alegría¹, Volkhard Kaefer², Patrick D. Curtis^{1*}

8

9

10 ¹Department of Biology, University of Mississippi, University, MS 38677, USA

11 ²Institute of Pharmacology, Research Core Unit Metabolomics, Hannover Medical School,

12 30625 Hannover, Germany

13

14

15

16 *Corresponding author. Mailing address: Department of Biology, University of Mississippi, 402

17 Shoemaker Hall, University, Mississippi 38677 USA. Phone: 662-915-1911. Fax: 662-915-

18 5144. Email: pdcurtis@olemiss.edu.

19

20

21 **Abstract**

22 The DivJ-DivK-PleC signaling system of *Caulobacter crescentus* is a signaling network
23 that regulates polar development and the cell cycle. This system is conserved in related bacteria,
24 including the sister genus *Brevundimonas*. Previous studies had shown unexpected phenotypic
25 differences between the *C. crescentus divK* mutant and the analogous mutant of *Brevundimonas*
26 *subvibrioides*, but further characterization was not performed. Here, phenotypic assays
27 analyzing motility, adhesion, and pilus production (the latter characterized by a newly discovered
28 bacteriophage) revealed that *divJ* and *pleC* mutants have mostly similar phenotypes as their *C.*
29 *crescentus* homologs, but *divK* mutants maintain largely opposite phenotypes than expected.
30 Suppressor mutations of the *B. subvibrioides divK* motility defect were involved in cyclic-di-
31 GMP (c-di-GMP) signaling, including the diguanylate cyclase *dgcB*, and *cleD* which is
32 hypothesized to affect flagellar function in a c-di-GMP dependent fashion. However, the screen
33 did not identify the diguanylate cyclase *pleD*. Disruption of *pleD* in *B. subvibrioides* caused no
34 change in *divK* or *pleC* phenotypes, but did reduce adhesion and increase motility of the *divJ*
35 strain. Analysis of c-di-GMP levels in these strains revealed incongruities between c-di-GMP
36 levels and displayed phenotypes with a notable result that suppressor mutations altered
37 phenotypes but had little impact on c-di-GMP levels in the *divK* background. Conversely, when
38 c-di-GMP levels were artificially manipulated, alterations of c-di-GMP levels in the *divK* strain
39 had minimal impact on phenotypes. These results suggest that DivK performs a critical function
40 in the integration of c-di-GMP signaling into the *B. subvibrioides* cell cycle.

41

42

43

44 **Importance**

45 Cyclic-di-GMP and associated signaling proteins are widespread in bacteria, but its role
46 in physiology is often complex and difficult to predict through genomic level analyses. In *C.*
47 *crescentus*, c-di-GMP has been integrated into the developmental cell cycle, but there is
48 increasing evidence that environmental factors can impact this system as well. The research
49 presented here suggests that the integration of these signaling networks could be more complex
50 than previously hypothesized, which could have a bearing on the larger field of c-di-GMP
51 signaling. In addition, this work further reveals similarities and differences in a conserved
52 regulatory network between organisms in the same taxonomic family, and the results show that
53 gene conservation does not necessarily imply close functional conservation in genetic pathways.

54 Introduction

55 Though model organisms represent a small portion of the biodiversity found on Earth, the
56 research that has resulted from their study shapes much of what we know about biology today.

57 The more closely related species are to a model organism, the more that theoretically can be
58 inferred about them using the information from the model organism. Modern genomic studies
59 have given this research an enlightening new perspective. Researchers can now compare the
60 conservation of particular systems genetically. Using model organisms can be a very efficient
61 and useful means of research, but the question still remains of how much of the information
62 gained from the study of a model can be extrapolated unto other organisms. Though genomic
63 comparison shows high levels of conservation between genes of different organisms, this does
64 not necessarily mean the function of those genes or systems has been conserved. This
65 phenomenon seems to be evident in the *Caulobacter crescentus* system.

66 *C. crescentus* is a Gram-negative alphaproteobacterium that lives a dimorphic lifestyle. It
67 has been used as a model organism for the study of cell cycle regulation, intracellular signaling,
68 and polar localization of proteins and structures in bacteria. The *C. crescentus* life cycle begins
69 with the presynthetic (G_1) phase in which the cell is a motile “swarmer cell” which contains a
70 single flagellum and multiple pili at one of the cell’s poles [for review, see (1)]. During this
71 period of the life cycle, the cell cannot replicate its chromosome or perform cell division. Upon
72 differentiation, the cell dismantles its pili and ejects its flagellum. It also begins to produce
73 holdfast, an adhesive polysaccharide, at the same pole from which the flagellum was ejected.
74 The cell then develops a stalk, projecting the holdfast away from the cell at the tip of the stalk.
75 The differentiation of the swarmer cell to the “stalked cell” marks the beginning of the synthesis
76 (S) phase of the cell life cycle as chromosome replication is initiated. As the stalked cell

77 replicates its chromosome and increases its biomass in preparation for cell division, it is referred
78 to as a predivisional cell. Toward the late predivisional stage, it again becomes replication
79 incompetent and enters the postsynthetic (G_2) phase of development. At the end of the G_2 phase,
80 the cell completes division forming two different cell types. The stalked cell can immediately
81 reenter the S phase, while the swarmer cell moves once again through the G_1 phase.

82 *Brevundimonas subvibrioides* is another Gram-negative alphaproteobacterium found in
83 oligotrophic environments that lives a dimorphic lifestyle like that of *C. crescentus*.

84 *Brevundimonas* is the next closest genus phylogenetically to *Caulobacter*. According to a
85 Pairwise Average Nucleotide Identity (ANI) test, their genomes are approximately 74% identical.
86 Bioinformatic analyses showed that all developmental signaling proteins found in the *C.*
87 *crescentus* cell cycle are conserved *B. subvibrioides* (2, 3). All the known developmental
88 regulators found in *C. crescentus* are also present in *B. subvibrioides*, and these regulators are
89 orthologs as they are bi-directional best hits when searched against each genome, and amino acid
90 identity is extremely high (3)(Supplementary Table S1). Conversely, no other proteins thought to
91 interact with DivK in more distantly related Alphaproteobacteria, such as PdhS1 or CbrA, are
92 apparent in the *B. subvibrioides* genome. However, little physiological characterization has
93 been performed. Conservation of genes does not necessarily mean conservation of function or
94 properties (3). Essential gene studies within the Alphaproteobacteria have shown that gene
95 essentiality/non-essentiality in one organism does not always correspond with that in another
96 organism (3-6). Analyses that have been performed on *C. crescentus* and *B. subvibrioides* have
97 shown many similarities in gene essentiality between the two, but have shown several surprising
98 differences as well (3).

99 In *C. crescentus*, the DivJ-DivK-PleC system controls the spatial activation of one of the
100 master regulators in *C. crescentus*, CtrA (1, 7). This system is a prime example of how *C.*
101 *crescentus* has evolved traditional two-component proteins into a more complex signaling
102 pathway and, as a result, has developed a more complex life cycle. The DivJ-DivK-PleC
103 pathway consists of two histidine kinases (PleC and DivJ) and a single response regulator (DivK)
104 (8, 9). DivJ is absent in swarmer cells but is produced during swarmer cell differentiation. It
105 then localizes to the stalked pole (8). DivJ is required for, among other things, proper stalk
106 placement and regulation of stalk length. *C. crescentus divJ* mutants display filamentous shape,
107 a lack of motility, and holdfast overproduction (8, 9).

108 PleC localizes to the flagellar pole during the predivisional cell stage (10). Though
109 structurally a histidine kinase PleC acts as a phosphatase, constitutively de-phosphorylating
110 DivK (8, 9). *C. crescentus pleC* mutants display a lack of pili, holdfast, and stalks, and have
111 paralyzed flagella leading to a loss of motility (11-13). DivK is a single-domain response
112 regulator (it lacks an output domain) whose location is dynamic throughout the cell cycle (9, 14).
113 DivK remains predominantly unphosphorylated in the swarmer cell, while it is found mostly in
114 its phosphorylated form in stalked cells. Photobleaching and FRET analysis show that DivK
115 shuttles rapidly back and forth from pole to pole in the pre-divisional cell depending on its
116 phosphorylation state (9). Previous studies have shown that phosphorylated DivK localizes
117 bipolarly while primarily unphosphorylated DivK is delocalized throughout the cell (9). A *divK*
118 cold-sensitive mutant suppresses the non-motile phenotype of *pleC* at 37°C. However, at 25°C,
119 it displays extensive filamentation much like the *divJ* mutant (15). Additionally, filamentous
120 *divK* mutants sometimes had multiple stalks, though the second stalk was not necessarily polar.

121 Furthermore, electron microscopy of *divK* disruption mutants led to the discovery that they lack
122 flagella.

123 Upon completion of cytokinesis, PleC and DivJ are segregated into different
124 compartments, thus DivK phosphorylation levels in each compartment are dramatically different.
125 This leads to differential activation of CtrA in the different compartments (9, 16). In the
126 swarmer cell, the de-phosphorylated DivK leads to the downstream activation of CtrA. CtrA in
127 its active form binds the chromosome at the origin of replication and prevents DNA replication
128 (17, 18). The opposite effect is seen in stalked cells where highly phosphorylated DivK results
129 in the inactivation of CtrA and, therefore, permits DNA replication (19).

130 Gene essentiality studies in *B. subvibrioides* led to the discovery of a discrepancy in the
131 essentiality of DivK. In *C. crescentus* DivK is essential for growth, while in *B. subvibrioides*
132 DivK is dispensable for growth (3, 15). Further characterization found dramatic differences in
133 the phenotypic consequences of disruption. Through the use of a cold-sensitive DivK allele or
134 by ectopic depletion, *C. crescentus divK* disruption largely phenocopies *divJ* disruption in cell
135 size and motility effects (8, 9, 15). This is to be expected as DivK~P is the active form and both
136 *divJ* or *divK* disruption reduce DivK~P levels. In *B. subvibrioides*, disruption of *divJ* leads to the
137 same effects in cell size, motility, and adhesion (3). However, *divK* disruption leads to opposite
138 phenotypes of cell size and adhesion, and while motility is impacted it is likely by a different
139 mechanism.

140 While the previous study revealed important differences between the organisms, it did not
141 analyze the impact of PleC disruption, nor did it examine pilus production or subcellular protein
142 localization. The work presented here further characterizes the DivJ-DivK-PleC signaling

143 system in *B. subvibrioides* and begins to address the mechanistic reasons for the unusual
144 phenotypes displayed by the *B. subvibrioides divK* mutant.

145

146 **Materials and Methods**

147 *Strains and growth conditions*

148 A complete list of strains used in this study is presented in the appendix (see
149 Supplementary Table S2). *Brevundimonas* strains were cultured at 30°C on PYE medium (2 g
150 peptone, 1 g yeast extract, 0.3 g MgSO₄ · 7H₂O, 0.735 CaCl₂) (20). Kanamycin was used at 20
151 µg/ml, gentamycin at 5 µg/ml, and tetracycline at 2 µg/ml when necessary. PYE plates
152 containing 3% sucrose were used for counter-selection. *Escherichia coli* was cultured on Luria-
153 Bertani (LB) medium (10 g/L tryptone, 10 g/L NaCl, 5 g/L yeast extract) at 37°C. Kanamycin
154 was used at 50 µg/ml, gentamycin at 20 µg/ml, and tetracycline at 12 µg/ml when necessary.

155

156 *Mutant generation*

157 The *B. subvibrioides* $\Delta divJ$, $\Delta divK$, and $\Delta divJ\Delta divK$ mutants were used from a previous
158 study (3). The *B. subvibrioides* $\Delta pleC$ construct was made by PCR amplifying an upstream
159 fragment of ~650 bps using primers PleC138Fwd
160 (attgaagccggetggcgccaCCAGATCGAAAAGGTGCAGCCC) and PleCdwRev
161 (tctagccgcGCCCCGCAAGGCGCTCTC) and a downstream fragment of ~550 bps using
162 primers PleCupFwd (cttgccggggcGCGGCCTAGAGCCGGTCA) and PleC138Rev
163 (cgtcacgcccgaagctagcggGTGCTGGGATGAAGACACG). The primers were designed using the
164 NEBuilder for Gibson Assembly tool online (New England Biolabs) and were constructed to be
165 used with the pNPTS138 vector (MRK Alley, unpublished). Following a digestion of the vector

166 using HindIII and EcoRI the vector along with both fragments were added to Gibson Assembly
167 Master Mix (New England Biolabs) and allowed to incubate for an hour at 50°C. Reactions
168 were then transformed into *E. coli* and correct plasmid construction verified by sequencing to
169 create plasmid pLAS1. This plasmid was used to delete *pleC* in *B. subvibrioides* as previously
170 described (3).

171 To create insertional mutations in genes, internal fragments from each gene were PCR
172 amplified. A fragment from gene *cpaF* was amplified using primers cpaFF
173 (GCGAACAGAGCGACTACTACCACG) and cpaFR (CCACCAGGTTCTTCATCGTCAGC).
174 A fragment from gene *pleD* was amplified using primers PleDF (CCGGCATGGACGGGTTC)
175 and PleDR (CGTTGACGCCAGTTCCAG). A fragment from gene *dgcB* was amplified using
176 primers DgcBF (GAGATGCTGGCGGCTGAATA) and DgcBR
177 (CGAACTCTTCGCCACCGTAG). A fragment from gene *cleD* was amplified using primers
178 Bresu1276F (ATCGCCGATCCGAACATGG) and Bresu1276R
179 (TTCTCGACCCGCTTGAACAG). The fragments were then cloned into the pCR vector using
180 the Zero Blunt cloning kit (Thermo Fisher), creating plasmids pPDC17 (*cpaF*), pLAS1 (*pleD*),
181 pLAS2 (*dgcB*), and pLAS3 (*cleD*). These plasmids were then transformed into *B. subvibrioides*
182 strains as previously published (3). The pCR plasmid is a non-replicating plasmid in *B.*
183 *subvibrioides* that facilitates insertion of the vector into the gene of interest via recombination,
184 thereby disrupting the gene.

185 To create a C-terminal *B. subvibrioides* DivJ fusion, ~50% of the *divJ* gene covering the
186 3' end was amplified by PCR using primers BSdivJgfpF
187 (CCTCATATGGGTTTACGGGGCCTACGGG) and BSdivJgfpR
188 (CGAGAATTCGAGACGGTCGGCGACGGTCCTG), and cloned into the pGFPC-2 plasmid

189 (21), creating plasmid pPDC11. To create a C-terminal *B. subvibrioides* PleC fusion, ~50% of
190 the *pleC* gene covering the 3' end was amplified by PCR using primers BSpleCgfpF
191 (CAACATATGCCAGAAGGACGAGCTGAACCGC) and BSpleCgfpR
192 (TTTGAATTCGAGGCCGCCCGCGCCTGTTGTTG), and cloned into the pGFPC-2 plasmid,
193 creating plasmid pPDC8. These plasmids are non-replicative in *B. subvibrioides* and therefore
194 integrate into the chromosome by homologous recombination at the site of each targeted gene.
195 The resulting integration creates a full copy of gene under the native promoter that produces a
196 protein with C-terminal GFP tag, and a ~50% 5' truncated copy with no promoter. This
197 effectively creates a strain where the tagged gene is the only functional copy.

198 Due to the small size of the *divK* gene, a region including the *divK* gene and ~500 bp of
199 sequence upstream of *divK* was amplified using primers BSdivKgfpF
200 (AGGCATATGCCAGCGACAGGGTCTGCACC) and BSdivKgfpR
201 (CGGGAATTCGATCCCGCCAGTACCGGAACGC) and cloned into pGFPC-2, creating
202 plasmid pPDC27. After homologous recombination into the *B. subvibrioides* genome, two
203 copies of the *divK* gene are produced, both under the native promoter, one of which encodes a
204 protein C-terminally fused to GFP.

205 Constructs expressing *E. coli ydeH* under IPTG induction on a medium copy (pTB4) and
206 low copy (pSA280) plasmids were originally published in (22). Constructs expressing
207 *Pseudomonas aeruginosa pchP* under vanillate induction (pBV-5295) as well as an active site
208 mutant (pBV-5295_{E328A}) were originally published in (23).

209

210 *Transposon mutagenesis*

211 Transposon mutagenesis was performed on the *B. subvibrioides* $\Delta divK$ mutant using the
212 EZ-Tn5 <KAN-2> TNP transposome (Epicentre). *B. subvibrioides* $\Delta divK$ was grown overnight
213 in PYE to an OD₆₀₀ of about 0.07 [quantified with a Thermo Nanodrop 2000 (Thermo Scientific)].
214 Cells (1.5 ml) were centrifuged 15,000 x g for 3 min at room temperature. The cell pellet was
215 then resuspended in 1 ml of water before being centrifuged again. This process was repeated.
216 Cells were resuspended in 50 μ l of nuclease free water, to which 0.2 μ l of transposome was
217 added. The mixture was incubated at room temperature for 10 minutes. The mixture was added
218 to a Gene Pulser Cuvette with a 0.1 cm electrode gap (Bio-Rad). The cells were then
219 electroporated as performed previously (3). Electroporation was performed using a GenePulser
220 Xcell (Bio-Rad) at a voltage of 1,500 V, a capacitance of 25 μ F, and a resistance of 400 Ω . After
221 electroporation, cells were resuspended with 1 ml of PYE then incubated shaking at 30°C for 3
222 hours. Cells were diluted 3-fold then spread on PYE + Kan plates (100 μ l/plate). Plates were
223 incubated at 30°C for 5-6 days.

224

225 *Swarm assay*

226 Strains were grown overnight in PYE, diluted to an OD₆₀₀ of 0.02, and allowed to grow
227 for two doublings (to OD₆₀₀ of ~0.06 - 0.07). All strains were diluted to OD₆₀₀ = 0.03 and 1 μ l of
228 culture was injected into a 0.3% agar PYE plate. Isopropyl 1-thio-b-D-galactopyranoside (IPTG)
229 (final concentration 1.5 mM) and vanillate (final concentration 1 mM) was added to plate
230 mixture before pouring plates where applicable. Molten 0.3% agar in PYE (25 ml) was poured
231 in each plate. Plates were incubated at 30°C for 5 days. Plates were imaged using a BioRad
232 ChemiDoc MP Imaging System with Image Lab software. Swarm size was then quantified in
233 pixels using ImageJ software. All swarm sizes on a plate were normalized to the wild-type

234 swarm on that plate. Assays were performed in triplicate and average and standard deviation
235 were calculated.

236

237 *Short-term adhesion assay*

238 Strains were grown overnight in PYE, diluted to an OD₆₀₀ of 0.02, and allowed to grow
239 for two doublings (to OD₆₀₀ of ~0.06 - 0.07). All strains were diluted to OD₆₀₀ = 0.05, at which
240 time 0.5 ml of each strain was inoculated into a well of a 24-well dish and incubated at 30°C for
241 2 hours in triplicate. Cell culture was removed and wells were washed 3 times with 0.5 ml of
242 fresh PYE. To each well was added 0.5 ml of 0.1% crystal violet and incubated at room
243 temperature for 20 minutes. Crystal violet was removed from each well before the plate was
244 washed by dunking in a tub of deionized water. Crystal violet bound to biomass was eluted with
245 0.5 ml acetic acid and the A₅₈₉ was quantified using a Thermo Nanodrop 2000 (Thermo
246 Scientific). Averages for each strain were calculated and then normalized to wild-type values
247 inoculated into the same plate. These assays were performed three times for each strain and used
248 to calculate average and standard deviation.

249

250 *Lectin-binding assay and microscopy conditions*

251 Holdfast staining was based on the protocol of (24). Strains of interest were grown
252 overnight in PYE to an OD₆₀₀ of 0.05 – 0.07. For each strain, 200 µl of culture were incubated
253 in a centrifuge tube with 2 µl of Alexafluor 488 (Molecular Probes) for 20 minutes at room
254 temperature. Cells were washed with 1 ml of sterile water then centrifuged 15,000 x g for 1 min
255 at room temperature. The cell pellet was resuspended in 30 µl of sterile water. A 1% agarose
256 pad (agarose in H₂O) was prepared for each strain on a glass slide to which 1 µl of culture was

257 added. Slides were then examined and photographed using an Olympus IX81 microscope by
258 phase contrast and epifluorescence microscopy using a 100X Plan APO oil immersion objective
259 The holdfast of GFP-labeled strains were stained with Alexafluor 594 conjugated to Wheat Germ
260 Agglutinin and prepared for imaging as described above. Alexafluor 488 and GFP labeled
261 strains were imaged with 470/20 nm excitation and 525/50 nm emission wavelengths.
262 Alexafluor 594 labeled strains were imaged with 572/35 nm excitation and 635/60 nm emission.

263

264 *Isolation of phage.*

265 Surface water samples from freshwater bodies were collected from several sources in
266 Lafayette County, Mississippi in 50 ml sterile centrifuge tubes and kept refrigerated. Samples
267 were passed through 0.45 μm filters to remove debris and bacterial constituents. To isolate
268 phage, 100 μl of filtered water was mixed with 200 μl mid-exponential *B. subvibrioides* cells and
269 added to 2.5 ml PYE with molten 0.5% agar. The solution was poured onto PYE agar plates,
270 allowed to harden, and then incubated at room temperature ($\sim 22^\circ\text{C}$) for 2 days. Plaques were
271 excised with a sterile laboratory spatula and placed into sterile 1.5 ml centrifuge tubes. 500 μl
272 PYE was added and the sample was refrigerated overnight to extract phage particles from the
273 agar. To build a more concentrated phage stock, the soft-agar plating was repeated with
274 extracted particles. Instead of excising plaques, 5 ml of PYE was added to the top of the plate
275 and refrigerated overnight. The PYE/phage solution was collected and stored in a foil-wrapped
276 sterile glass vial, and 50 μl chloroform was added to kill residual bacterial cells. Phage solutions
277 were stored at 4°C .

278

279 *Isolation of phage resistant mutants.*

280 *B. subvibrioides* was mutagenized with EZ-Tn5 transposome as described above. After
281 electroporation, cells were grown for 3 hr without selection, followed by 3 hr with kanamycin
282 selection. Transformed cells (100 μ l) were mixed with 100 μ l phage stock ($\sim 1 \times 10^{10}$ pfu/ml)
283 and plated on PYE agar medium with kanamycin. Colonies arose after ~ 5 days and were
284 transferred to fresh plates. Transformants had their genomic DNA extracted using the Bactozol
285 kit (Molecular Research Center). Identification of the transposon insertion sites was performed
286 using Touchdown PCR (25), with transposon specific primers provided in the EZ-Tn5 kit.

287

288 *Phage sensitivity assays.*

289 Two different phage sensitivity assays were used. First (hereafter referred to as the
290 spotting assay) involved the mixing of cells and phage in liquid suspension and then spotting
291 droplets on an agar surface. Each cell culture was normalized to $OD_{600} = 0.03$. The culture was
292 then diluted 10^{-2} , 10^{-4} and 10^{-5} in PYE medium. For control assays, 5 μ l of each cell suspension
293 (including undiluted) was mixed with 5 μ l PYE, then 5 μ l of this mixture was spotted onto PYE
294 plates, allowed to dry, then incubated at room temperature for 2 days. For the phage sensitivity
295 assays, 5 μ l of each cell suspension was mixed with 5 μ l of phage stock ($\sim 1 \times 10^{10}$ pfu/ml), 5 μ l
296 spotted onto PYE plates, allowed to dry, then incubated at room temperature for 2 days.

297 The second assay (hereafter referred to as the soft agar assay) involved creating a lawn of
298 cells and spotting dilutions of phage on the lawn. Cell cultures were normalized to $OD_{600} = 0.03$
299 and 200 μ l of cells were mixed with 4.5 ml PYE with molten 0.5% agar, mixed, poured onto a
300 PYE agar plate, and allowed to harden. Phage stock ($\sim 1 \times 10^{10}$ pfu/ml) was diluted in PYE
301 media as individual 10X dilutions to a total of 10^{-7} dilution. 5 μ l of each phage concentration

302 (10^{-1} to 10^{-7} , 7 concentrations total) were spotted on top of the soft agar surface and allowed to
303 dry. Plates were incubated 2 days at room temperature.

304

305 *Swarm suppressor screen*

306 Individual colonies from a transposon mutagenesis were collected on the tip of a thin
307 sterile stick and inoculated into a 0.3% agar PYE plate. Wild-type *B. subvibrioides* strains as
308 well as *B. subvibrioides* $\Delta divK$ were inoculated into each plate as controls. 32 colonies were
309 inoculated into each plate including the 2 controls. Plates were incubated at 30°C for 5 days.
310 Plates were then examined for strains that had expanded noticeably further than the parent *divK*
311 strain from the inoculation point. Those strains of interest were then isolated for further testing.

312

313 *Identification of swarm suppressor insertion sites.*

314 Swarm suppressor insertion sites were identified by Inverse PCR (iPCR, (26)). Genomic
315 DNA (gDNA) was purified using the DNeasy Blood & Tissue Kit (Qiagen). Digests were then
316 prepared using 1 μ g of gDNA and either AluI or HhaI incubated overnight at 37°C. Digests were
317 heat inactivated for 20 minutes at 80°C then column cleaned using the DNA Clean and Concen-
318 trator kit (Zymo Research). Dilute ligations (100-500 ng DNA) were then prepared so that di-
319 gested fragments would likely circularize. Ligations were incubated at 17°C overnight. Reac-
320 tions were heat inactivated at 65°C for 20 minutes then column cleaned using the DNA Clean
321 and Concentrator kit. The ligated DNA was used as the template in a PCR reaction with primers
322 that anneal inside the transposon sequence. Primers used included AluIF (GCGTT-
323 GCCAATGATGTTACAGATGAG) and AluIR (GCCCCGACATTATCGCGAGCCC) as well as
324 HhaIF2 (TTACGCTGACTTGACGGGAC) and HhaIR2 (GGAGAAAACCTCACCGAGGCA).

325 Given the large size of the resulting AluI fragment from the transposon sequence alone, another
326 primer AluIFSeq (CGGTGAGTTTTCTCCTTCATTACAG) was designed specifically for se-
327 quencing after iPCR was complete. Primers were designed facing outward toward either end of
328 the transposon such that the resulting PCR amplicon would be fragments that begin and end with
329 transposon sequence with gDNA in between. PCR reactions were prepared using 10.75 μ l H₂O,
330 5 μ l HF buffer (BioRad), 5 μ l combinational enhancer solution (2.7 M betaine, 6.7 mM DTT,
331 6.7% DMSO, 55 μ g/mL BSA), 1 μ l of template DNA from each ligation, 1 μ l each of their re-
332 spective forward and reverse primers (primers based on what enzyme was used during diges-
333 tion), 1 μ l of 10 mM dNTP's (BioLine), and 0.25 μ l iProof (BioRad). PCR conditions were as
334 follows. Initial melt was set to 98°C for 30 seconds. Melting temperature was set to 98°C for 45
335 seconds, annealing temperature was set to 52°C for 20 seconds, extension temperature was set to
336 72°C for 2:30 seconds. and these three steps were cycled through 30 times. Final extension tem-
337 perature was set to 72°C for 10 minutes. 5 μ l from each reaction were run on a 1% agarose gel
338 to check for fragments. Those reactions that tested positive for bands were drop dialyzed using
339 0.025 μ m membrane filters (Millipore) then prepared for sequencing with their respective pri-
340 mers. Samples were sent to Eurofins for sequencing.

341

342 *Quantification of c-di-GMP.*

343 Strains of interest were grown overnight in PYE to an OD₆₀₀ of 0.05 – 0.07. Metabolites
344 were then extracted from each sample and c-di-GMP was quantified using the protocol previous-
345 ly described in (27). Metabolites from each strain were extracted in triplicate. Remaining cellu-
346 lar material was dried at room temperature and resuspended in 800 μ L 0.1M NaOH. Samples
347 were incubated at 95°C for 15 minutes. Samples were then centrifuged for 10 min at 4°C,

348 20,800 x g. Protein levels were measured in triplicate for each sample using 10 μ l from the pel-
349 let treatment and the Pierce BCA Protein Assay Kit (Thermo Fisher Scientific). Intracellular
350 concentrations measured by mass spectrometry were then normalized to protein levels.

351

352 Results

353 **Deletion mutants in the *B. subvibrioides* DivJ-DivK-PleC system result in varied**
354 **phenotypes compared to that of analogous *C. crescentus* mutations.** In the previous study
355 done in *Brevundimonas subvibrioides*, deletion mutants of the genes *divJ*, *divK*, and a *divJdivK*
356 double mutant were made and partially characterized, uncovering some starkly different
357 phenotypes compared to the homologous mutants in *C. crescentus*. However, characterization of
358 this system was not complete as it did not extend to a key player in this system: PleC. As
359 previously mentioned, *C. crescentus pleC* mutants display a lack of motility, pili, holdfast, and
360 stalks (28). To begin examining the role of PleC in *B. subvibrioides*, an in-frame deletion of the
361 *pleC* gene (Bresu_0892) was created. This strain, along with the previously published *divJ*,
362 *divK*, and *divJdivK* strains, were used in a swarm assay to analyze motility. All mutant strains
363 displayed reduced motility in swarm agar compared to the wild-type (Figure 1A, Supplemental
364 Figure S1). This had been reported for the published strains (3). The mechanistic reasons for
365 this are unclear. All were observed to produce flagella and were seen to swim when observed
366 microscopically. The *divJ* strain has significantly filamentous cell shape which is known to
367 inhibit motility through soft agar, but the *divK* and *divJdivK* strains actually have shorter than
368 wild-type cells. The nature of the *pleC* motility defect is also unknown. The cell size of the *pleC*
369 mutants was not noticeably different from that of wild-type cells (Figure 1B). The *C. crescentus*
370 *pleC* mutant is known to have a paralyzed flagellum which leads to a null motility phenotype,

371 but *B. subvibrioides pleC* mutants were observed swimming under the microscope suggesting
372 that unlike *C. crescentus* their flagellum remains functional. While the mechanistic reason for
373 this discrepancy is unknown, it does provide another important difference in developmental
374 signaling mutants between the two organisms.

375 To further the phenotypic characterization, these strains were analyzed for the surface
376 adhesion properties using both a short-term adhesion assay as well as staining holdfast material
377 with a fluorescently-conjugated lectin. As previously reported, the *divK* and *divJdivK* strains had
378 minimal adhesion and no detectable holdfast material (Figure 1AB). It was previously reported
379 that the *divJ* strain had increased adhesion over wild-type, but in this study, it was found to have
380 slightly reduced adhesion compared to wild-type. It is not clear if this difference in results
381 between the two studies is significant. The *pleC* strain had reduced adhesion compared to wild-
382 type, but more adhesion compared to the *divK* or *divJdivK* strains. When analyzed by
383 microscopy, the *pleC* strain was found to still produce detectable holdfast (Figure 1B,
384 Supplemental Figure S2), which is a difference from the *C. crescentus pleC* strain where holdfast
385 was undetectable (28, 29).

386 An important component to the function of this signaling system is the subcellular
387 localization of DivJ and PleC to the stalked and flagellar poles respectively. As the localization
388 of these proteins had yet to be characterized in *B. subvibrioides*, GFP-tagged constructs were
389 generated such that the tagged versions were under native expression. Because *B. subvibrioides*
390 cells very rarely produce stalks under nutrient-replete conditions (30), holdfast material was
391 stained using a WGA lectin conjugated with a fluorophore that uses RFP imaging conditions.
392 When the *divJ-gfp* strain was analyzed (N = 403 cells), the majority of cells (82.9%) had no
393 detectable signal (Figure 1C). It is not clear if this means the cells are not producing DivJ or that

394 the level is below the detection limit. When cells had detectable fluorescence it was seen only as
395 a unipolar focus (17.1%). When cells had detectable DivJ-GFP foci and labeled holdfast, the
396 foci were found exclusively at the holdfast pole (N = 55 cells). When the *pleC-GFP* strain was
397 imaged (N = 433 cells), most cells displayed a unipolar focus (68.8%). Only 28.9% of cells
398 displayed no fluorescence. A small number of cells (2.3%) had seemingly bipolar PleC
399 localization; these cells may be transitioning from the swarmer to stalked state. Of the cells that
400 had detectable PleC-GFP foci and labeled holdfast (N = 38), all PleC-GFP foci were found at the
401 pole opposite the holdfast (Figure 1C, Supplemental Figure S3). As it has been demonstrated
402 that holdfast material is produced at the same pole as the stalk in *B. subvibrioides* (30), this result
403 suggests that these proteins demonstrate the same localization patterns as their *C. crescentus*
404 counterparts. DivK-GFP was seen to form different localization patterns in different cells
405 (Figure 1C, Supplemental Figure S4). Of the 431 cells counted, the vast majority (85.8%)
406 showed total cell fluorescence with no distinct localization. Bipolar localization was seen in
407 6.3% of cells, and unipolar localization was seen in 7.9% of cells. Of the cells that displayed
408 unipolar localization and a detectable holdfast, DivK-GFP was localized almost exclusively to
409 the stalked pole (96.3%, N = 27). These results contrast *C. crescentus* results in some ways. In
410 *C. crescentus* DivK-GFP was found predominantly bipolarly localized (56%), with 12%
411 displayed stalked pole localization and 32% displaying no detectable fluorescence (31), though
412 this quantification was performed using stalked cells specifically. Diffuse total body
413 fluorescence was not reported in that study, but it is known that DivK-GFP is diffuse in swarmer
414 cells. It should be noted that the work in *C. crescentus* expressed *divK-gfp* from a low copy
415 plasmid using the native promoter, while here a plasmid integration scheme was used to create a
416 merodiploid; however, both strains had both tagged and untagged versions of *divK* each

417 expressed by native promoters, so it is not clear if strain construction is the cause of the
418 differences in localization pattern. Therefore, DivJ and PleC localizations match the *C.*
419 *crenscentus* model, while DivK appears to spend most of the time delocalized (with some bipolar
420 and stalked pole localization), as opposed to *C. crescentus* where the protein appears to spend
421 most of the time bipolarly localized. This is another case where the histidine kinase results
422 somewhat match between organisms, while the response regulator results are quite different.

423 **Isolation of a bacteriophage capable of infecting *B. subvibrioides*.** Another important
424 developmental event in *C. crescentus* is the production of pili at the flagellar pole coincident
425 with cell division. Pili are very difficult to visualize, and in *C. crescentus* the production of pili
426 in strains of interest can be assessed with the use of the bacteriophage Φ CbK, which infects the
427 cell using the pilus. Resistance to the phage indicates the absence of pili. However,
428 bacteriophage that infect *C. crescentus* do not infect *B. subvibrioides* (data not shown) despite
429 their close relation. In an attempt to develop a similar tool for *B. subvibrioides*, a phage capable
430 of infecting this organism was isolated.

431 Despite the fact that *B. subvibrioides* was isolated from a freshwater pond in California
432 over 50 years ago, a phage capable of infecting the bacterium was isolated from a freshwater
433 pond in Lafayette County, Mississippi. This result is a testament to the ubiquitous nature of
434 *Caulobacter* and *Brevundimonas* species in freshwater environments all over the globe. This
435 phage has been named Delta, after the state's famous Mississippi Delta region. To determine the
436 host range for this phage, it was tested against multiple *Brevundimonas* species (Figure 2A).
437 Delta has a relatively narrow host range, causing the largest reduction of cell viability in *B.*
438 *subvibrioides* and *B. aveniformis*, with some reduction in *B. basaltis* and *B. halotolerans* as well.
439 None of the other 14 *Brevundimonas* species showed any significant reduction in cell viability.

440 Neither did Delta show any infectivity toward *C. crescentus* (data not shown). While *B.*
441 *subvibrioides*, *B. aveniformis*, and *B. basaltis* all belong to the same sub-clade within the
442 *Brevundimonas* genus (P. Caccamo, Y.V. Brun, personal communication), so do *B.*
443 *kwangchunensis*, *B. alba* and *B. lenta*, all of which are more closely related to *B. subvibrioides*
444 than *B. aveniformis* and all of which were resistant to the phage. Therefore, infectivity does not
445 appear to fall along clear phylogenetic lines and may be determined by some other factor.

446 To begin identifying the infection mechanism of Delta, *B. subvibrioides* was randomly
447 mutagenized with a Tn5 transposon and resulting transformants were mixed with Delta to select
448 for transposon insertions conferring phage resistance as a way to identify the phage infection
449 mechanism. Phage resistant mutants were readily obtained and maintained phage resistance
450 when rescreened. A number of transposon insertion sites were sequenced and several were
451 found in the pilus biogenesis cluster homologous to the *C. crescentus flp*-type pilus cluster. In-
452 sertions were found in the homologs for *cpaD*, *cpaE* and *cpaF*; it is known disruption of *cpaE* in
453 *C. crescentus* abolishes pilus formation and leads to Φ CbK resistance (31-33). A targeted dis-
454 ruption was made in *cpaF* and tested for phage sensitivity by the soft agar assay (Figure 2B).
455 The *cpaF* disruption caused complete resistance to the phage. The fact that multiple transposon
456 insertions were found in the pilus cluster and that the *cpaF* disruption leads to phage resistance
457 strongly suggest that Delta utilizes the *B. subvibrioides* pilus as part of its infection mechanism.
458 The identification of another pili-tropic phage is not surprising as pili are major phage targets in
459 multiple organisms.

460 Phage Delta was used to assess the potential pilus production in developmental signaling
461 mutants using the soft agar assay (Figure 2C). The *divJ* mutant has similar susceptibility to
462 Delta as the wild-type, suggesting this strain still produces pili. This result is consistent with the

463 *C. crescentus* result as the *C. crescentus divJ* mutant is Φ CbK susceptible (8). Conversely, the *B.*
464 *subvibrioides pleC* mutant shows a clear reduction in susceptibility to Delta, indicating that this
465 strain is deficient in pilus production. If so, this would also be consistent with the *C. crescentus*
466 *pleC* mutant which is resistant to Φ CbK (8, 28). With regards to the *divK* strain, if that mutant
467 was to follow the *C. crescentus* model it should demonstrate the same susceptibility as the *divJ*
468 strain. Alternatively, as the *divK* strain has often demonstrated opposite phenotypes to *divJ* in *B.*
469 *subvibrioides*, one might predict it to demonstrate resistance to Delta. As seen in Figure 2C, the
470 *divK* strain (and the *divJdivK* strain) shows the same level of resistance to phage Delta as the
471 *pleC* mutant. Therefore, in regards to phage sensitivity, the *divK* strain is once again opposite of
472 the prediction of the *C. crescentus* model. Interestingly, none of these developmental signaling
473 mutants demonstrate complete resistance to Delta as seen in the *cpaF* strain. This result suggests
474 that these mutations impact pilus synthesis, but do not abolish it completely.

475 **A suppressor screen identifies mutations related to c-di-GMP signaling.** As the *B.*
476 *subvibrioides divK* mutant displays the most unusual phenotypes with regard to the *C. crescentus*
477 model, this strain was selected for further analysis. Complementation of *divK* was attempted by
478 expressing wild-type DivK from an inducible promoter on a replicating plasmid, however
479 induction failed to complement any of the *divK* phenotypes (data not shown), indicating proper
480 complementation conditions have not yet been identified. Transposon mutagenesis was
481 performed on this strain and mutants were screened for those that restore motility. Two mutants
482 were found (Bresu_1276 and Bresu_2169) that restored motility to the *divK* strain, and
483 maintained this phenotype when recreated by plasmid insertional disruption. Both mutants were
484 involved in c-di-GMP signaling. The *C. crescentus* homolog of the Bresu_1276 gene, CC3100
485 (42% identical to Bresu_1276), was recently characterized in a subcluster of CheY-like response

486 regulators and renamed CleD (34). Function of CleD is, at least in part, initiated by binding c-di-
487 GMP via an arginine-rich residue with high affinity and specificity for c-di-GMP. Upon binding,
488 roughly 30% of CleD localizes to the flagellated pole of the swarmer cell. Nesper et. al suggests
489 that CleD may bind directly to the flagellar motor switch protein, FliM. In *E. coli* and
490 *Salmonella*, the flagellar brake protein YcgR interacts with FliM in a c-di-GMP dependent
491 manner, biasing the motor in the smooth-running counter clockwise direction (35, 36), but YcgR
492 is not a response regulator-type protein, and no obvious YcgR homologs are present in the *C.*
493 *crenscentus* or *B. subvibrioides* genomes (data not shown). Based upon the *C. crescentus*
494 findings, it was hypothesized that increased c-di-GMP levels cause activation of CleD, which
495 binds to the flagellar switch and inhibits flagellar function (34). In *C. crescentus*, *cleD* mutants
496 are 150% more motile while their adhesion does not differ significantly from that of the wild-
497 type. Unlike conventional response regulators, the phosphoryl-receiving aspartate is replaced
498 with a glutamate in CleD. In other response regulators, replacement of the aspartate with a
499 glutamate mimics the phosphorylated state and locks the protein in an active conformation.
500 Alignment of CleD with orthologs from various *Caulobacter* and *Brevundimonas* species
501 demonstrated that this was a conserved feature of CleD within this clade (Figure 3). Similar to
502 *C. crescentus*, the swarm size of *B. subvibrioides cleD* mutant increased to 151% compared to
503 wild-type. A knockout of *cleD* in the *divK* background led to a complete restoration of motility
504 compared to that of wild-type, while adhesion did not appear to be affected (Figure 4A). These
505 phenotypes correspond relatively well with the model given in Nesper et al. As CleD is thought
506 to inhibit motor function, a cell lacking CleD would have less motor inhibition, leading to an
507 increase in motility and a delay in surface attachment, though *cleD* disruption had no impact on

508 the phage sensitivity phenotypes of the wild-type or *divK*-derived strains (Supplemental Figure
509 S5).

510 Bresu_2169 is the homolog of the well-characterized *C. crescentus* diguanylate cyclase,
511 DgcB (61% identical amino acid sequence). In *C. crescentus*, DgcB is one of two major
512 diguanylate cyclases that work in conjunction to elevate c-di-GMP levels which in turn helps
513 regulate the cell cycle, specifically in regards to polar morphogenesis (37). It has been shown
514 that a *dgcB* mutant causes adhesion to drop to nearly 50% compared to wild-type while motility
515 was elevated to almost 150%. It was unsurprising to find very similar changes in phenotypes in
516 the *dgcB* mutant in wild-type *B. subvibrioides*. In the *dgcB* mutant, swarm expansion increased
517 by 124% while adhesion dropped to only 46% compared to wild-type (Figure 4A). Though the
518 *dgcB* mutant did not restore motility to wild-type levels in the *divK* background, the insertion did
519 cause the swarm to expand nearly twice as much as that of the *divK* parent. These phenotypes
520 are consistent with our current understanding of c-di-GMP's role in the *C. crescentus* cell cycle.
521 As c-di-GMP builds up in the cell, it begins to make the switch from its motile phase to its
522 sessile phase. Deleting a diguanylate cyclase therefore should prolong the swarmer cell stage,
523 thereby increasing motility and decreasing adhesion. Similar to *cleD*, *dgcB* disruption had no
524 impact on the phage sensitivity phenotypes of the wild-type or *divK*-derived strains
525 (Supplemental Figure S5).

526 ***A pleD* mutant lacks hypermotility in *divK* background.** Given the identification of
527 *dgcB* in the suppressor screen, it was of note that the screen did not identify the other well-
528 characterized diguanylate cycle involved in the *C. crescentus* cell cycle, PleD. PleD is an
529 atypical response regulator with two receiver domains in addition to the diguanylate cyclase
530 domain (38, 39). The *pleD* mutant in *C. crescentus* has been shown to suppresses the *pleC*

531 motility defect in *C. crescentus* which led to its initial discovery alongside *divK* (22, 38, 39).
532 However, in a wild-type background, *pleD* disruption has actually been shown to reduce motility
533 to about 60% compared to wild-type (22, 37). Additionally, a 70% reduction in adhesion is
534 observed in *pleD* mutants which is thought to be a result of delayed holdfast production (22, 37,
535 40). Therefore, it was not clear whether a *pleD* disruption would lead to motility defect
536 suppression in a *divK* background. To examine this, a *pleD* disruption was made in both the
537 wild-type and *divK B. subvibrioides* strains (Figure 4A). The *divK* and *pleD* genes belong to the
538 same two gene operon, where *divK* is the first gene. As previously published, deletion of *divK*
539 was performed using an in-frame deletion and thus is not expected to impact *pleD* expression.
540 As *pleD* is the latter of the two genes, plasmid insertion into *pleD* is not expected to impact *divK*
541 expression.

542 In wild-type *B. subvibrioides*, *pleD* disruption resulted in little change to motility with
543 swarms expanding to 105% of wild-type, while adhesion dropped to only 10% compared to
544 wild-type. While this data supports the broader theory of c-di-GMP's role as the "switch"
545 between the motile and sessile phase of the cell cycle, it does not align with those phenotypes
546 seen in a *C. crescentus pleD* mutant. While adhesion is reduced in both organisms, the reduction
547 in adhesion was much more drastic in *B. subvibrioides* than *C. crescentus*. Moreover, the
548 motility phenotypes in homologous *pleD* mutants do not match. In *C. crescentus*, *pleD* mutants
549 causes a decrease in motility by nearly 40% in the wild-type background (22, 37). In *B.*
550 *subvibrioides*, motility is the same as wild-type (Figure 4A). Disruption of *pleD* also causes a
551 reduction in phage sensitivity (Figure 7B, Supplemental Figure S5).

552 Another interesting detail discovered in performing these assays was the lack of change
553 in phenotypes seen in the *pleD* disruption in a *divK* background. It is not surprising that

554 adhesion was not negatively impacted as it is already significantly lower in the *divK* strain
555 compared to wild-type. However, disrupting the *pleD* gene did not increase motility in the *divK*
556 mutant. In fact, motility was reduced to 89% compared to the *divK* control (Figure 4A).
557 Additionally, both *divK* and *pleD* mutants had the same reduction in phage sensitivity as the *divK*
558 *pleD* double mutant (Figure 7B, Supplemental Figure S5). It is not clear why disruption of the
559 diguanylate cyclase DgcB leads to increased motility in both the wild-type and *divK*
560 backgrounds, but disruption of another diguanylate cycle PleD does not increase motility in
561 either background. Interestingly, it was previously shown that DivJ and PleC do not act on DivK
562 alone, but in fact also have the same enzymatic functions on PleD phosphorylation as well (41).
563 It may be that PleD acts upon motility not through c-di-GMP signaling but instead by modulating
564 DivK activity, perhaps by interacting/interfering with the polar kinases. If so, then the absence
565 of DivK could block this effect.

566 **Suppressor mutants have altered c-di-GMP levels.** As these mutations are all involved
567 in c-di-GMP signaling, c-di-GMP levels in each strain were quantified to determine if the cellular
568 levels in each strain correspond to observed phenotypes. These metabolites were quantified from
569 whole cell lysates. In bacteria, high c-di-GMP levels typically induce adhesion while low c-di-
570 GMP levels induce motility. Therefore, it would be expected that hypermotile strains would
571 show decreased c-di-GMP levels. Instead, hypermotile strains of the wild-type background had
572 varying c-di-GMP levels (Figure 4B). The *pleD* knockout had reduced c-di-GMP levels as
573 predicted. While it may seem surprising that c-di-GMP levels are not affected in a *dgcB* mutant,
574 this in fact true of the *C. crescentus* mutant as well (37). This result suggests that the c-di-GMP
575 levels found in the *dgcB* strain do not appear to be the cause for the observed changes in motility

576 and adhesion. A comparison of c-di-GMP levels and phenotypic analyses between the organisms
577 is presented in Table 1.

578 Perhaps the most interesting result is that the *cleD* mutant had the highest c-di-GMP
579 levels of all strains tested. This is surprising as it is suggested by Nesper et. al. that CleD does
580 not affect c-di-GMP levels at all, but rather is affected by them. CleD is a response regulator that
581 contains neither a GGDEF nor an EAL domain characteristic of diguanylate cyclases and
582 phosphodiesterases respectively. Instead it is thought CleD binds to c-di-GMP, which then
583 stimulates it to interact with the flagellar motor. The data presented here suggests that there may
584 be a feedback loop whereby increased motility in the swarm agar leads to increased c-di-GMP
585 levels. One potential explanation is that this situation increases contact with surfaces. Yet the
586 *cleD* mutant clearly shows decreased adhesion compared to wild-type despite the elevated c-di-
587 GMP levels. Therefore, there must be a block between the high c-di-GMP levels and the
588 execution of those levels into adhesion in this strain.

589 Very different results were obtained when c-di-GMP levels were measured in *divK*
590 derived strains (Figure 4B). While a wide variety of motility phenotypes were observed in *cleD*,
591 *dgcB*, and *pleD* disruptions in the *divK* background, their c-di-GMP levels are all nearly identical
592 to that of the *divK* mutant. For the *dgcB divK* strain, once again the increase in motility occurs
593 without a change in c-di-GMP levels. These results suggest that DgcB is not a significant
594 contributor to c-di-GMP production in *B. subvibrioides*. While *pleD* disruption leads to
595 decreased c-di-GMP levels in the wild-type background, no change is seen in the *divK*
596 background. This means in the absence of PleD some other enzyme must be responsible for
597 achieving these levels of c-di-GMP. Given the lack of impact DgcB seems to have on c-di-GMP
598 signaling, it is tempting to speculate an as-yet characterized diguanylate cyclase is involved.

599 Lastly the elevated c-di-GMP levels seen in the *cleD* disruption are not seen when *cleD* is
600 disrupted in the *divK* background. This result suggests that whatever feedback mechanism leads
601 to elevated c-di-GMP levels is not functional in the *divK* mutant.

602 **Non-native diguanylate cyclases and phosphodiesterases cause shifts in c-di-GMP**
603 **levels but do not alter phenotypes in the *divK* strain.** As previously mentioned, c-di-GMP is
604 thought to assist in the coordination of certain developmental processes throughout the cell cycle.
605 The previous results found mutations in genes involved in c-di-GMP signaling could suppress
606 developmental defects, but the actual effect of the mutations appears uncoupled from effects on
607 c-di-GMP levels. In order to further investigate the connection between developmental defects
608 and c-di-GMP signaling, c-di-GMP levels were artificially manipulated. Plasmid constructs
609 expressing non-native c-di-GMP metabolizing enzymes previously used in similar experiments
610 in *C. crescentus* were obtained and expressed in *B. subvibrioides*. The diguanylate cyclase *ydeH*
611 from *Escherichia coli* was expressed from two different IPTG inducible plasmids; a medium
612 copy number pBBR-based plasmid, pTB4, and a low copy number pRK2-based plasmid, pSA280
613 (22). The combination of the two different inducible copy number plasmids resulted in different
614 elevated levels of c-di-GMP (Figure 5B). A phosphodiesterase *pchP* from *Pseudomonas*
615 *aeruginosa* (42), as well as its active site mutant *pchP*^{E328A} were expressed from pBV-MCS4, a
616 vanillate inducible medium copy number plasmid (23). The phosphodiesterase on a medium
617 copy plasmid was enough to decrease levels of c-di-GMP to either equivalent or lower levels as
618 is seen in the *divK* strain. The decrease was not observed when the active site mutant was
619 expressed, demonstrating that the reduction of c-di-GMP was the result of *pchP* expression.
620 Wild-type and *divK* strains were grown with IPTG and vanillate respectively to control for any
621 growth effects caused by the inducers.

622 Expression of the phosphodiesterase in the wild-type background caused a reduction in c-
623 di-GMP which would be predicted to increase motility and decrease adhesion. While this strain
624 had a large reduction of adhesion, it also had a small reduction in motility (Figure 5A).
625 However, these same results were obtained when this construct was expressed in wild-type *C.*
626 *crenscentus* (22). It is interesting to note, though, that expression of the phosphodiesterase results
627 in similar c-di-GMP levels to that of the *divK* strain yet the phosphodiesterase strain
628 demonstrates much larger swarm sizes than the *divK* strain. The low copy diguanylate cyclase
629 plasmid did not appear to affect c-di-GMP levels (Figure 5B), and unsurprisingly did not appear
630 to affect either motility or adhesion. However, the medium copy diguanylate cyclase plasmid
631 increased c-di-GMP levels but had surprising phenotypic results. An increase in c-di-GMP
632 levels would be predicted to increase adhesion and decrease motility. When this construct was
633 expressed in wild-type *C. crescentus* there was a small decrease to adhesion but a very large
634 decrease in motility, almost to the point of non-motility (22); the motility results mirror the
635 prediction based on c-di-GMP levels. In *B. subvibrioides* the same construct produced a slight
636 decrease to adhesion, but motility actually increased instead of drastically decreasing. Here not
637 only do *B. subvibrioides* results differ from *C. crescentus* results, but the results contradict
638 predictions based on known c-di-GMP paradigms.

639 In the *divK* background strain, expression of either diguanylate cyclase increases c-di-
640 GMP levels, though the low copy diguanylate cyclase increase is not as dramatic as the medium
641 copy. However, neither expression level has a significant impact on motility or adhesion (Figure
642 5). Neither the phosphodiesterase nor its active site mutant cause a noticeable shift in the c-di-
643 GMP levels compared to the *divK* strain nor any noticeable impact on phenotype. In fact, though
644 the c-di-GMP levels differed dramatically between strains, the phenotypes of all six of these

645 strains are not impacted. T-tests performed between each strain and its respective control
646 showed no significant difference. These results appear to be the antithesis of those found from
647 the suppressor screen. While the suppressor mutants showed recovery in their motility defect
648 compared to *divK*, their c-di-GMP levels did not significantly differ from each other or *divK*.
649 Conversely, when c-di-GMP levels were artificially manipulated, alterations of c-di-GMP levels
650 in the *divK* strain had no impact on phenotypes. These results suggest that DivK is somehow
651 serving as a block or a buffer to c-di-GMP levels and their effects on phenotypes and calls into
652 question the role c-di-GMP has in *B. subvibrioides* developmental progression.

653 **Disruption of *pleD* in developmental signaling mutants does not alter *pleC***
654 **phenotypes, but does alter *divJ* phenotypes.** As discussed above, disruption of *pleD* does not
655 impact the adhesion or swarm expansion phenotypes of a *divK* mutant. To determine the
656 epistatic relationship between *pleD* and other developmental signaling mutants of *B.*
657 *subvibrioides*, the *pleD* disruption was placed in the *divJ*, *divJdivK*, and *pleC* strains and
658 resultant mutants were analyzed for developmental defects (Figures 6 and 7). Disruption of *pleD*
659 does not alter the phenotypes of the *divK* or *divJdivK* strains in swarm expansion, adhesion,
660 holdfast formation, or phage sensitivity. The exception to this is the *divJdivK pleD::pCR* strain
661 which had a small but statistically significant reduction in adhesion compared to the *divJdivK*
662 parent ($p = 0.03$). These results are to be expected given previous results and the fact that the
663 *divJdivK* strain has consistently phenocopied the *divK* strain. What was not expected was that
664 disruption of *pleD* had no effect on *pleC* strain phenotypes. The *pleD* gene was originally
665 discovered as a motility suppressor of the *C. crescentus pleC* mutant (13), but in *B. subvibrioides*
666 *pleD* disruption does not alter any of the developmental phenotypes of the *pleC* strain. Instead,
667 *pleD* disruption alters some, but not all, of the *divJ* mutant phenotypes. The *divJ pleD::pCR*

668 strain had wild-type levels of phage sensitivity just like the *divJ* parent, and microscopic
669 examination of the strain also revealed the strain had a filamentous cell morphology
670 characteristic of the *divJ* parent strain (Figure 7A). However, this strain had a significant
671 reduction in adhesion, holdfast was undetectable, and there was a small but statistically
672 significant increase in motility. Essentially, *pleD* disruption removes holdfast formation and
673 increases motility without affecting cell filamentation or pilus production, though swarm
674 expansion results are clouded by the filamentous cell morphology which impacts swarm
675 expansion independent of flagellum function or chemotaxis. These *divJ pleD::pCR* results stand
676 in stark contrast to the *divJdivK* results where all developmental phenotypes copy the *divK*
677 phenotypes. Perhaps this suggests that PleD may have a more specific role in the morphological
678 changes that occur during *B. subvibrioides* cell cycle progression.

679

680 Discussion

681 Across closely related bacterial species, high levels of gene conservation are commonly
682 observed. It has therefore been a long-standing assumption that information gathered from
683 studying a model organism can be extrapolated to other closely related organisms. Through this
684 study, by comparing and contrasting the developmental signaling systems of *C. crescentus* and *B.*
685 *subvibrioides*, it has been shown that these assumptions may not be as safe to make as previously
686 thought. Preliminary data raised a few questions by demonstrating major differences in the
687 phenotypes of *divK* mutants between species. Here the system was analyzed in greater depth in
688 *B. subvibrioides* by examining subcellular protein localization, developmental phenotypes of a
689 *pleC* mutant, and isolating a pilitropic bacteriophage to examine pilus production in multiple
690 developmental mutants. GFP tagging revealed that the subcellular localization patterns of DivJ

691 and PleC in *B. subvibrioides* are consistent with the *C. crescentus* proteins. DivJ was
692 consistently detected at the holdfast (i.e. stalked) pole, while PleC was consistently detected at
693 the non-holdfast (i.e. flagellar) pole. DivK was found in a variety of localization patterns. In *C.*
694 *crescentus*, DivK is localized to the stalked pole in stalked cells, bi-polarly localized in
695 predivisional cells, and delocalized in swarmer cells. In *B. subvibrioides*, stalked pole and
696 bipolar localizations were observed, but the majority of cells displayed delocalized DivK-GFP.
697 If *B. subvibrioides* adhered to the *C. crescentus* model, this would suggest that over 85% of the
698 *B. subvibrioides* population in a growing culture is swarmer cells. Many of the cells with
699 delocalized DivK were in rosettes and/or had detectable holdfast (Supplemental Figure S4,
700 additional data not shown). Correlated with this is the fact that 82.9% of cells had no detectable
701 DivJ-GFP foci, while only 28.9% lacked detectable PleC-GFP foci; the presence of PleC and the
702 absence of DivJ would theoretically lead to complete dephosphorylation of DivK, which causes
703 delocalization in *C. crescentus*, such as in swarmer cells (43). This suggests that many, if not
704 most, *B. subvibrioides* stalked cells have delocalized DivK. One unusual facet of *B.*
705 *subvibrioides* physiology is the fact that the doubling time of this organism in PYE is 6.5 hours
706 (3), compared to the 1.5 hours of *C. crescentus* in the same media. It is not clear how the cell
707 cycle is adjusted to account for this longer generation time. Perhaps the *B. subvibrioides*
708 signaling system is held in a more swarmer cell like state even though the cells are
709 morphologically more like a stalked cell. However, stalked pole localization is observed, so
710 what induces the transition from delocalized to localized? More careful dissection of the *B.*
711 *subvibrioides* cell cycle, with particular respect to signaling protein localization, may reveal the
712 answer.

713 While the discovery that developmental protein localization in *B. subvibrioides* largely
714 matches the localization in *C. crescentus* may not be surprising, this discovery makes the
715 phenotypic results even more surprising (summarized in Table 2). Previously it was shown that
716 the *B. subvibrioides divJ* mutant closely matches the phenotypes of the *C. crescentus divJ* mutant
717 in regards to cell filamentation, holdfast production, adhesion and motility (3). Here pilus
718 synthesis was added by the use of a novel bacteriophage, and here still *B. subvibrioides divJ*
719 mirrored the *C. crescentus* results. In *C. crescentus divK* disruption/depletion leads to G1 cell
720 stage arrest (15); i.e. in the stalked cell stage prior to entering the predivisional stage. As a
721 consequence, the cells become extremely filamentous and do not produce flagella or pili. While
722 adhesion of this strain was never tested, cells are seen to produce stalks that touch tip to tip in
723 the rosette fashion, suggesting holdfast production. These phenotypes are similar to *divJ*
724 phenotypes, which makes sense given both mutations ultimately lead to lower levels of DivK~P.
725 Conversely, previously it was shown that *B. subvibrioides divK* deletion produced opposite
726 phenotypic results in cell size, holdfast production and adhesion. Both mutants were
727 compromised in motility, but the mechanistic reasons are unclear, especially given both strains
728 produce apparently functional flagella, though the morphology defects of the *divJ* strain may
729 have a bearing on these results. Here another difference was demonstrated between the strains as
730 the *B. subvibrioides divK* strain had an intermediate phage resistance phenotype. While *B.*
731 *subvibrioides divJ* largely matched *C. crescentus divJ*, and *B. subvibrioides* was largely opposite
732 *C. crescentus divK*, *B. subvibrioides pleC* was an intermediate of *C. crescentus pleC*. In *C.*
733 *crescentus pleC* mutants have normal cell size, but produce no pili, no holdfast (and thus are
734 adhesion deficient), and are non-motile due to a paralyzed flagellum. Here it was found that *B.*
735 *subvibrioides pleC* mutants have an intermediate phage resistance phenotype, suggesting

736 intermediate pilus production, intermediate adhesion with weak holdfast detection, and
737 intermediate motility. Therefore, comparing signaling mutants between organisms results in the
738 same, opposite, or intermediate results. These results are all the more confusing given the fact
739 that localization patterns of the proteins are mostly conserved between the organisms. It seems
740 unlikely that the phenotypic consequences are a result of altered localization patterns. This
741 suggests that the phenotypic consequences are a product of altered downstream signaling. Even
742 in *C. crescentus*, the exact connection between signaling protein disruption and phenotypic
743 consequence are largely unknown. Careful mapping of the signaling systems between the
744 mutation and the eventual phenotype is required in both organisms.

745 In an attempt to further map this system in *B. subvibrioides*, a suppressor screen was
746 employed using the *divK* mutant as its phenotypes differed most dramatically from its *C.*
747 *crescentus* homolog. Suppressor mutations were found in genes predicted to encode proteins
748 that affected or were affected by c-di-GMP. This was not necessarily a surprising discovery. C-
749 di-GMP is a second messenger signaling system conserved across many bacterial species used to
750 coordinate the switch between motile and sessile lifestyles. Previous research in *C. crescentus*
751 suggests that organism integrated c-di-GMP signaling into the swarmer-to-stalked cell transition.
752 Mutations that modify c-di-GMP signaling would be predicted to impact the swarmer cell stage,
753 perhaps lengthening the amount of time the cell stays in that stage and thus lead to an increase in
754 swarm spreading in soft agar. However, further inquiry into c-di-GMP levels of *divK* suppressor
755 mutants revealed discrepancies between c-di-GMP levels and their corresponding phenotypes.
756 Firstly, CleD, a CheY-like response regulator that is thought to affect flagellar motor function,
757 caused the strongest suppression of the *divK* mutant restoring motility levels to that of wild-type.
758 Given that the reported function of CleD is to bind the FlIM filament of the flagellar motor and

759 interfere with motor function to boost rapid surface attachment (34), it is expected that disruption
760 of *cleD* would result in increased motility and decreased adhesion which can be seen in both the
761 wild-type and *divK* background strains (Figure 4A). What was unexpected, however, was to find
762 that a lack of CleD led to one of the highest detected levels of c-di-GMP in this study, which was
763 surprising given that CleD has no predicted diguanylate cyclase or phosphodiesterase domains.
764 Yet when this same mutation was placed in the *divK* background, the c-di-GMP levels were
765 indistinguishable from the *divK* parent. Therefore, the same mutation leads to hypermotility in
766 two different backgrounds despite the fact that c-di-GMP levels are drastically different.
767 Consequently, the phenotypic results of the mutation do not match the c-di-GMP levels,
768 suggesting that c-di-GMP has little or no effect on the motility phenotype. A similar result was
769 seen with DgcB. Disruption of *dgcB* in either the wild-type or *divK* background resulted in
770 hypermotility, but c-di-GMP levels were not altered. Once again, the effect on motility occurred
771 independently of c-di-GMP levels. Disruption of *divK* seems to somehow stabilize c-di-GMP
772 levels. Even when non-native enzymes are expressed in the *divK* background the magnitude of
773 changes seen in the c-di-GMP pool is dampened compared to the magnitude of change seen
774 when the enzymes are expressed in the wild-type background. This may explain why *pleD* was
775 not found in the suppressor screen. While CleD and DgcB seem involved in c-di-GMP
776 signaling, their effect on the cell appears c-di-GMP-independent, while PleD appears to perform
777 its action by affecting the c-di-GMP pool. If that pool is stabilized in the *divK* strain, then
778 disruption of *pleD* will have no effect on either the c-di-GMP pool or on the motility phenotype.
779 However, it should be noted that c-di-GMP levels were measured from whole cell lysates and
780 does not reflect the possibility of spatial or temporal variations of c-di-GMP levels within the

781 cell. It is possible that CleD and DgcB have c-di-GMP dependent effects, but those effects are
782 limited to specific sub-cellular locations in the cell.

783 In *C. crescentus*, c-di-GMP is implicated in the morphological changes that occur during
784 swarmer cell differentiation, but c-di-GMP levels are also tied to the developmental network, and
785 more specifically CtrA activation, by two different mechanisms. First, through most of the cell
786 cycle the diguanylate cyclase DgcB is antagonized by the phosphodiesterase PdeA such that no
787 c-di-GMP is produced by DgcB (37). Upon swarmer cell differentiation PdeA is targeted for
788 proteolysis, leaving DgcB activity unchecked. This, combined with active PleD, increases c-di-
789 GMP levels in the cell. The elevated levels activate the protein PopA, which targets CtrA for
790 proteolysis, which is useful for swarmer cell differentiation as it will relieve the inhibition of
791 chromosome replication initiation performed by CtrA binding at the origin of replication. In the
792 second mechanism, it has been found that c-di-GMP is an allosteric regulator of CckA, the
793 hybrid histidine kinase responsible for phosphorylation of CtrA (44). As stated above, DivJ and
794 PleC have the same antagonistic phosphorylation activities on PleD as they do on DivK, and
795 phosphorylation induces PleD activity. During swarmer cell differentiation, isolated PleC is
796 replaced at the transitioning stalked pole by DivJ, and which leads to elevated PleD
797 phosphorylation and therefore higher enzymatic activity. This, combined with unchecked DgcB
798 activity, increases c-di-GMP levels which has been shown to inhibit kinase activity and stimulate
799 phosphatase activity of CckA, causing CtrA to be dephosphorylated and therefore deactivated.
800 Additionally, the same CckA phosphatase activity causes dephosphorylation of CpdR, which also
801 targets CtrA for proteolysis. It has also been shown that CpdR activity targets PdeA for
802 degradation, thereby permitting unchecked DgcB activity. Therefore, the elevation of c-di-GMP
803 levels during swarmer cell differentiation works redundantly to deactivate CtrA, which is

804 necessary for cell cycle progression, and serves to coordinate the morphological changes of
805 swarmer cell differentiation with the necessary changes in the signaling state of the
806 developmental network.

807 However, these models do not adequately explain some of the more unusual results
808 reported in this study. First, it is not clear why c-di-GMP levels appear stabilized in a *divK*
809 mutant in *B. subtilis*. In *C. crescentus* DivK has been shown to be an allosteric effector of
810 PleC, where non-phosphorylated DivK stimulates PleC to become a kinase and increase PleD~P
811 levels (45), though it is thought this activity only occurs during the onset of swarmer cell
812 differentiation. If one were to assume that DivK-driven PleC phosphorylation of PleD were the
813 sole mechanism of PleD phosphorylation, then theoretically the absence of DivK could mean
814 PleD is never phosphorylated and therefore c-di-GMP levels would not change above
815 background in a *divK* strain, but this would mean 1) observed DivJ kinase activity on PleD is
816 unimportant to PleD activity and it is only the phosphorylation of PleD by PleC (at the onset or
817 swarmer cell differentiation) that is important, and 2) PleD is the sole contributor to c-di-GMP
818 elevation and thus DgcB activity is not a meaningful contributor to measurable c-di-GMP
819 changes. Perhaps this second point is supported by our data here which shows a disconnect
820 between phenotype and c-di-GMP levels in *dgcB* mutants, and it was seen both here in *B.*
821 *subtilis* and in *C. crescentus* that overall c-di-GMP levels do not change much in *dgcB*
822 mutants (37). These models also do not explain why *pleD* disruption alters the adhesion
823 phenotypes of a *divJ* mutant. Assuming that DivJ is the PleD kinase, then PleD should be
824 inactive in a *divJ* strain and therefore disrupting *pleD* in a *divJ* background should have no effect.
825 In this study, it clearly does. Perhaps this result supports a hypothesis that only PleC
826 phosphorylation of PleD is biologically relevant. Additionally, assuming another PleD kinase is

827 active in a *divJ* strain, the results of *pleD* disruption should be redundant to *divJ* deletion, not
828 counter-productive. A *divJ* deletion should lead to decreased levels of DivK~P, which should
829 allow promiscuous interaction between DivL and CckA, ultimately leading to over-activation of
830 CtrA. Disruption of *pleD* should lead to decreased c-di-GMP levels (which was seen in this
831 study) which would not direct CckA into its phosphatase role, and also potentially lead to over-
832 activation of CtrA. Therefore, combining *divJ* and *pleD* mutations should be redundant, if not
833 additive. Yet in this study it was seen *pleD* disruption reversed the holdfast formation and
834 motility of the *divJ* strain. Even further, *pleD* disruption did not alter the cell filamentation or
835 pilus production of the *divJ* strain, which may suggest that PleD's role in cell cycle progression
836 is specific to holdfast and/or motility and argues against a role in CtrA regulation.

837 This research raises several questions. First, what is the exact role of c-di-GMP in cell
838 cycle progression of *B. subtilis*? Is this signal a major driver of the swarmer cell and
839 swarmer cell differentiation? Or have the various c-di-GMP signaling components found new
840 roles in the swarmer cell and the actual c-di-GMP is simply vestigial. What is the role of PleD in
841 cell cycle progression? Why are c-di-GMP levels so stable when DivK is removed? And lastly,
842 are the answers to these questions specific to *B. subtilis*, or can they be extrapolated back
843 to *C. crescentus*? Further investigation into c-di-GMP signaling in both organisms is required.

844

845 **Acknowledgements**

846 The authors wish to thank P. Caccamo and Y.V. Brun for providing most of the
847 *Brevundimonas* species, as well as the iPCR protocol that had been adapted for use in *C.*
848 *crescentus*, U. Jenal for providing several plasmids, Satish Adhikari and Kari Ferolito for their

849 help with cloning, and the Curtis lab for general support. This work was supported by the United
850 States National Science Foundation CAREER program award 1552647.

851

852

853

854 **References**

- 855 1. **Curtis PD, Brun YV.** 2010. Getting in the loop: regulation of development in
856 *Caulobacter crescentus*. *Microbiol Mol Biol Rev* **74**:13-41.
- 857 2. **Brilli M, Fondi M, Fani R, Mengoni A, Ferri L, Bazzicalupo M, Biondi EG.** 2010.
858 The diversity and evolution of cell cycle regulation in alpha-proteobacteria: a
859 comparative genomic analysis. *BMC Syst Biol* **4**:52.
- 860 3. **Curtis PD, Brun YV.** 2014. Identification of essential alphaproteobacterial genes reveals
861 operational variability in conserved developmental and cell cycle systems. *Mol Microbiol*
862 **93**:713-735.
- 863 4. **Brassinga AK, Siam R, McSween W, Winkler H, Wood D, Marczynski GT.** 2002.
864 Conserved response regulator CtrA and IHF binding sites in the alpha-proteobacteria
865 *Caulobacter crescentus* and *Rickettsia prowazekii* chromosomal replication origins. *J*
866 *Bacteriol* **184**:5789-5799.
- 867 5. **Barnett MJ, Hung DY, Reisenauer A, Shapiro L, Long SR.** 2001. A homolog of the
868 CtrA cell cycle regulator is present and essential in *Sinorhizobium meliloti*. *J Bacteriol*
869 **183**:3204-3210.
- 870 6. **Lang AS, Beatty JT.** 2000. Genetic analysis of a bacterial genetic exchange element: the
871 gene transfer agent of *Rhodobacter capsulatus*. *Proc Natl Acad Sci U S A* **97**:859-864.
- 872 7. **Goley ED, Iniesta AA, Shapiro L.** 2007. Cell cycle regulation in *Caulobacter*: location,
873 location, location. *J Cell Sci* **120**:3501-3507.
- 874 8. **Wheeler RT, Shapiro L.** 1999. Differential localization of two histidine kinases
875 controlling bacterial cell differentiation. *Mol Cell* **4**:683-694.
- 876 9. **Matroule JY, Lam H, Burnette DT, Jacobs-Wagner C.** 2004. Cytokinesis monitoring
877 during development; rapid pole-to-pole shuttling of a signaling protein by localized
878 kinase and phosphatase in *Caulobacter*. *Cell* **118**:579-590.
- 879 10. **Deich J, Judd EM, McAdams HH, Moerner WE.** 2004. Visualization of the movement
880 of single histidine kinase molecules in live *Caulobacter* cells. *Proc Natl Acad Sci U S A*
881 **101**:15921-15926.
- 882 11. **Ely B, Gerardot CJ, Fleming DL, Gomes SL, Frederikse P, Shapiro L.** 1986. General
883 nonchemotactic mutants of *Caulobacter crescentus*. *Genetics* **114**:717-730.
- 884 12. **Fukuda A, Asada M, Koyasu S, Yoshida H, Yaginuma K, Okada Y.** 1981. Regulation
885 of polar morphogenesis in *Caulobacter crescentus*. *J Bacteriol* **145**:559-572.
- 886 13. **Sommer JM, Newton A.** 1989. Turning off flagellum rotation requires the pleiotropic
887 gene *pleD*: *pleA*, *pleC*, and *pleD* define two morphogenic pathways in *Caulobacter*
888 *crescentus*. *J Bacteriol* **171**:392-401.
- 889 14. **Cabantous S, Guillet V, Ohta N, Newton A, Samama JP.** 2002. Characterization and
890 crystallization of DivK, an essential response regulator for cell division and
891 differentiation in *Caulobacter crescentus*. *Acta Crystallogr D Biol Crystallogr* **58**:1249-
892 1251.
- 893 15. **Hecht GB, Lane T, Ohta N, Sommer JM, Newton A.** 1995. An essential single domain
894 response regulator required for normal cell division and differentiation in *Caulobacter*
895 *crescentus*. *EMBO J* **14**:3915-3924.
- 896 16. **Biondi EG, Reisinger SJ, Skerker JM, Arif M, Perchuk BS, Ryan KR, Laub MT.**
897 2006. Regulation of the bacterial cell cycle by an integrated genetic circuit. *Nature*
898 **444**:899-904.

- 899 17. **Quon KC, Yang B, Domian IJ, Shapiro L, Marczynski GT.** 1998. Negative control of
900 bacterial DNA replication by a cell cycle regulatory protein that binds at the chromosome
901 origin. *Proc Natl Acad Sci U S A* **95**:120-125.
- 902 18. **Bastedo DP, Marczynski GT.** 2009. CtrA response regulator binding to the *Caulobacter*
903 chromosome replication origin is required during nutrient and antibiotic stress as well as
904 during cell cycle progression. *Mol Microbiol* **72**:139-154.
- 905 19. **Domian IJ, Quon KC, Shapiro L.** 1997. Cell type-specific phosphorylation and
906 proteolysis of a transcriptional regulator controls the G1-to-S transition in a bacterial cell
907 cycle. *Cell* **90**:415-424.
- 908 20. **Poindexter JS.** 1964. Biological properties and classification of the *Caulobacter* group.
909 *Bacteriol Rev* **28**:231-295.
- 910 21. **Thanbichler M, Iniesta AA, Shapiro L.** 2007. A comprehensive set of plasmids for
911 vanillate- and xylose-inducible gene expression in *Caulobacter crescentus*. *Nucleic Acids*
912 *Res* **35**:e137.
- 913 22. **Abel S, Bucher T, Nicollier M, Hug I, Kaefer V, Abel Zur Wiesch P, Jenal U.** 2013.
914 Bi-modal distribution of the second messenger c-di-GMP controls cell fate and
915 asymmetry during the *Caulobacter* cell cycle. *PLoS Genet* **9**:e1003744.
- 916 23. **Duerig A, Abel S, Folcher M, Nicollier M, Schwede T, Amiot N, Giese B, Jenal U.**
917 2009. Second messenger-mediated spatiotemporal control of protein degradation
918 regulates bacterial cell cycle progression. *Genes Dev* **23**:93-104.
- 919 24. **Janakiraman RS, Brun YV.** 1999. Cell cycle control of a holdfast attachment gene in
920 *Caulobacter crescentus*. *J Bacteriol* **181**:1118-1125.
- 921 25. **Levano-Garcia J, Verjovski-Almeida S, da Silva AC.** 2005. Mapping transposon
922 insertion sites by touchdown PCR and hybrid degenerate primers. *BioTechniques* **38**:225-
923 229.
- 924 26. **Ochman H, Gerber AS, Hartl DL.** 1988. Genetic applications of an inverse polymerase
925 chain reaction. *Genetics* **120**:621-623.
- 926 27. **Burhenne H, Kaefer V.** 2013. Quantification of cyclic dinucleotides by reversed-phase
927 LC-MS/MS. *Methods in molecular biology* **1016**:27-37.
- 928 28. **Wang SP, Sharma PL, Schoenlein PV, Ely B.** 1993. A histidine protein kinase is
929 involved in polar organelle development in *Caulobacter crescentus*. *Proc Natl Acad Sci*
930 *U S A* **90**:630-634.
- 931 29. **Smith CS, Hinz A, Bodenmiller D, Larson DE, Brun YV.** 2003. Identification of genes
932 required for synthesis of the adhesive holdfast in *Caulobacter crescentus*. *J Bacteriol*
933 **185**:1432-1442.
- 934 30. **Curtis PD.** 2017. Stalk formation of *Brevundimonas* and how it compares to *Caulobacter*
935 *crescentus*. *PloS one* **12**:e0184063.
- 936 31. **Curtis PD, Quardokus EM, Lawler ML, Guo X, Klein D, Chen JC, Arnold RJ, Brun**
937 **YV.** 2012. The scaffolding and signalling functions of a localization factor impact polar
938 development. *Mol Microbiol* **84**:712-735.
- 939 32. **Curtis PD, Klein D, Brun YV.** 2013. Effect of a *ctrA* promoter mutation, causing a
940 reduction in CtrA abundance, on the cell cycle and development of *Caulobacter*
941 *crescentus*. *BMC microbiology* **13**:166.
- 942 33. **Skerker JM, Shapiro L.** 2000. Identification and cell cycle control of a novel pilus
943 system in *Caulobacter crescentus*. *EMBO J* **19**:3223-3234.
- 944 34. **Nesper J, Hug I, Kato S, Hee CS, Habazettl JM, Manfredi P, Grzesiek S, Schirmer**

- 945 **T, Emonet T, Jenal U.** 2017. Cyclic di-GMP differentially tunes a bacterial flagellar
946 motor through a novel class of CheY-like regulators. *Elife* **6**.
- 947 35. **Fang X, Gomelsky M.** 2010. A post-translational, c-di-GMP-dependent mechanism
948 regulating flagellar motility. *Mol Microbiol* **76**:1295-1305.
- 949 36. **Paul K, Nieto V, Carlquist WC, Blair DF, Harshey RM.** 2010. The c-di-GMP binding
950 protein YcgR controls flagellar motor direction and speed to affect chemotaxis by a
951 "backstop brake" mechanism. *Mol Cell* **38**:128-139.
- 952 37. **Abel S, Chien P, Wassmann P, Schirmer T, Kaever V, Laub MT, Baker TA, Jenal U.**
953 2011. Regulatory cohesion of cell cycle and cell differentiation through interlinked
954 phosphorylation and second messenger networks. *Mol Cell* **43**:550-560.
- 955 38. **Hecht GB, Newton A.** 1995. Identification of a novel response regulator required for the
956 swarmer-to-stalked-cell transition in *Caulobacter crescentus*. *J Bacteriol* **177**:6223-6229.
- 957 39. **Aldridge P, Paul R, Goymer P, Rainey P, Jenal U.** 2003. Role of the GGDEF regulator
958 PleD in polar development of *Caulobacter crescentus*. *Mol Microbiol* **47**:1695-1708.
- 959 40. **Levi A, Jenal U.** 2006. Holdfast formation in motile swarmer cells optimizes surface
960 attachment during *Caulobacter crescentus* development. *J Bacteriol* **188**:5315-5318.
- 961 41. **Skerker JM, Prasol MS, Perchuk BS, Biondi EG, Laub MT.** 2005. Two-component
962 signal transduction pathways regulating growth and cell cycle progression in a bacterium:
963 a system-level analysis. *PLoS Biol* **3**:e334.
- 964 42. **Massimelli MJ, Beassoni PR, Forrellad MA, Barra JL, Garrido MN, Domenech CE,
965 Lisa AT.** 2005. Identification, cloning, and expression of *Pseudomonas aeruginosa*
966 phosphorylcholine phosphatase gene. *Current microbiology* **50**:251-256.
- 967 43. **Jacobs C, Hung D, Shapiro L.** 2001. Dynamic localization of a cytoplasmic signal
968 transduction response regulator controls morphogenesis during the *Caulobacter* cell
969 cycle. *Proc Natl Acad Sci U S A* **98**:4095-4100.
- 970 44. **Lori C, Ozaki S, Steiner S, Bohm R, Abel S, Dubey BN, Schirmer T, Hiller S, Jenal
971 U.** 2015. Cyclic di-GMP acts as a cell cycle oscillator to drive chromosome replication.
972 *Nature* **523**:236-239.
- 973 45. **Paul R, Jaeger T, Abel S, Wiederkehr I, Folcher M, Biondi EG, Laub MT, Jenal U.**
974 2008. Allosteric regulation of histidine kinases by their cognate response regulator
975 determines cell fate. *Cell* **133**:452-461.
- 976 46. **Gonin M, Quardokus EM, O'Donnol D, Maddock J, Brun YV.** 2000. Regulation of
977 stalk elongation by phosphate in *Caulobacter crescentus*. *J Bacteriol* **182**:337-347.
- 978 47. **Pierce DL, O'Donnol DS, Allen RC, Javens JW, Quardokus EM, Brun YV.** 2006.
979 Mutations in DivL and CckA rescue a *divJ* null mutant of *Caulobacter crescentus* by
980 reducing the activity of CtrA. *J Bacteriol* **188**:2473-2482.
- 981 48. **Reisinger SJ, Huntwork S, Viollier PH, Ryan KR.** 2007. DivL performs critical cell
982 cycle functions in *Caulobacter crescentus* independent of kinase activity. *J Bacteriol*
983 **189**:8308-8320.
- 984 49. **Tsokos CG, Perchuk BS, Laub MT.** 2011. A Dynamic Complex of Signaling Proteins
985 Uses Polar Localization to Regulate Cell-Fate Asymmetry in *Caulobacter crescentus*.
986 *Developmental cell* **20**:329-341.
- 987 50. **Aldridge P, Jenal U.** 1999. Cell cycle-dependent degradation of a flagellar motor
988 component requires a novel-type response regulator. *Mol Microbiol* **32**:379-391.

989

991 **Table 1: Comparison of changes in c-di-GMP levels and phenotypes between *C. crescentus***
 992 **and *B. subvibrioides* strains.**

Mutation	Organism ¹	Phenotype ²			References
		c-di-GMP	Adhesion	Motility	
<i>cleD</i>	<i>C.c.</i>	N.D.	+/- ³	++	(34)
	<i>B.s.</i>	++ (193%)	+/-	++	This study
<i>dgcB</i>	<i>C.c.</i>	+ (~105%)	+/-	++	(37)
	<i>B.s.</i>	+ (108%)	+/-	++	This study
<i>pleD</i>	<i>C.c.</i>	+/- (~70%)	+/-	+/-	(37)
	<i>B.s.</i>	- (27%)	+/-	+	This study

993 ¹ *C.c.* = *C. crescentus*, *B.s.* = *B. subvibrioides*.

994 ² ++ = above wild-type levels, + = wild-type or near wild-type levels, +/- below wild-type or
 995 intermediate levels, - = null or near null levels, N.D. = not determined.

996 ³ Adhesion was measured of individual cells in microfluidic devices.

997

998 **Table 2: Comparison of developmental mutation phenotypes between *C. crescentus* and *B.***
 999 ***subvibrioides*.**

Mutation	Organism ²	Phenotype ¹					References
		Cell Size	Adhesion	Holdfast	Motility	Pili	
<i>divJ</i>	<i>C.c.</i>	Filament	++	++	-	+	(8, 46, 47)
	<i>B.s.</i>	Filament	+ / ++	++	-	+	(3), this study
<i>divK</i>	<i>C.c.</i>	Filament	N.D. ³	N.D. ³	-	-	(15, 48, 49)
	<i>B.s.</i>	Short	-	-	-	+/-	(3), this study
<i>pleC</i>	<i>C.c.</i>	Normal	-	-	-	-	(12, 13, 23, 28, 29)
	<i>B.s.</i>	Normal	+/-	+/-	+/-	+/-	This study
<i>pleD</i>	<i>C.c.</i>	Normal	-	+	+/-	+	(23, 37, 39, 40, 50)
	<i>B.s.</i>	Normal	-	-	+	+/-	This study
<i>dgcB</i>	<i>C.c.</i>	Normal	+/-	+	++	N.D.	(37)
	<i>B.s.</i>	Normal	+/-	+	++	+	This study

1000 ¹ ++ = above wild-type levels, + = wild-type or near wild-type levels, +/- below wild-type or
 1001 intermediate levels, - = null or near null levels, N.D. = not determined.

1002 ² *C.c.* = *C. crescentus*, *B.s.* = *B. subvibrioides*.

1003 ³ Adhesion and holdfast production were not analyzed in this strain, but circumstantial evidence
 1004 suggests holdfast material is produced.

1005

1006 **Figure Legends**

1007 **Figure 1. Deletions in *B. subvibrioides* developmental signaling genes results in varying**

1008 **physiological phenotypes.** A) Wild-type, *divJ*, *divK*, *divJdivK*, and *pleC* *B. subvibrioides* strains

1009 were analyzed for swarm expansion (dark bars) and adhesion (light bars) defects using a soft

1010 agar swarm assay and a short-term adhesion assay. Mutant strains were normalized to wild-type

1011 results for both assays. Deletion of *divJ* gives motility defects but minimal adhesion defects,

1012 similar to *C. crescentus divJ* results. *B. subvibrioides divK* and *divJdivK* strains give opposite

1013 results, with severe motility and adhesion defects. The *B. subvibrioides pleC* strain has reduced

1014 motility and moderately reduced adhesion, which is similar but not identical to the *C. crescentus*

1015 *pleC* strain. B) Lectin staining of holdfast material of wild-type, *divJ*, *divK*, *divJdivK*, and *pleC*

1016 strains. The *pleC* strain, despite having reduced adhesion in the short-term adhesion assay, still

1017 has detectable holdfast material C) GFP-tagged DivJ localizes to the holdfast producing pole,

1018 while PleC-GFP localizes to the pole opposite the holdfast. DivK-GFP displays bi-polar

1019 localization. These localization patterns are identical those of *C. crescentus* homologs.

1020

1021 **Figure 2. Bacteriophage Delta serves as a tool to investigate *B. subvibrioides* pilus**

1022 **production.** A) Phage Delta was tested for infection in 18 different *Brevundimonas* species.

1023 Control assays used PYE media instead of phage stock. Delta caused a significant reduction in

1024 *B. subvibrioides* and *B. aveniformis* viability, with some reduction in *B. basaltis* and *B.*

1025 *halotolerans* as well. B) Phage Delta was tested against wild-type and *cpaF*::pCR *B.*

1026 *subvibrioides* strains using a soft agar phage assay. Wild-type displayed zones of clearing with

1027 phage dilutions up to 10^{-7} , while the *cpaF* strain showed resistance to all phage dilutions. C) *B.*

1028 *subvibrioides* developmental signaling mutants were tested with phage Delta in soft agar phage

1029 assays. Wild-type shows clear susceptibility to Delta, as does the *divJ* strain suggesting that, like
1030 *C. crescentus divJ*, it produces pili. The *pleC* strain shows a 2-3 orders of magnitude reduced
1031 susceptibility to the phage, indicating reduced pilus production which is consistent with the *C.*
1032 *crescentus* phenotype. The *divK* and *divJdivK* strains display similar to resistance as the *pleC*
1033 strain. Here again, *divK* disruption causes the opposite phenotype to *divJ* disruption, unlike the
1034 *C. crescentus* results.

1035

1036 **Figure 3. CleD displays a conserved glutamate residue in place of an aspartate typical of**
1037 **response regulators.** CleD orthologs from various Caulobacter and Brevundimonas species
1038 were aligned by ClustalW, along with *B. subvibrioides* DivK. The shaded box indicates *B.*
1039 *subvibrioides* DivK D53, which is analogous to *C. crescentus* DivK D53 and is the known
1040 phosphoryl-accepting residue. This alignment demonstrates that CleD orthologs all contain a
1041 glutamate substitution at that site, which has been found to mimic the phosphorylated state and
1042 lock the protein in an active conformation in other response regulators.

1043

1044 **Figure 4. Phenotypes exhibited by *divK* suppressors do not coincide with intracellular c-di-**
1045 **GMP levels.** A) Swarm expansion (dark bars) and surface adhesion (light bars) of suppressor
1046 mutations tested in both the wild-type and *divK* background. Disruption of CleD, DgcB and
1047 PleD lead to increased motility in the wild-type background, but only CleD and DgcB lead to
1048 increased motility in the *divK* background. Disruptions in the wild-type background lead to
1049 varying levels of adhesion reduction, but the same disruptions had no effect on adhesion in the
1050 *divK* background. * indicates that motility is statistically insignificant from the *divK* parent,
1051 while ** indicates motility is statistically significant from the *divK* parent ($p < 0.05$). B) C-di-

1052 GMP levels were measured using mass spectrometry then normalized to the amount of biomass
1053 from each sample. Despite disruptions causing increased motility in the wild-type background,
1054 those strains had different c-di-GMP levels. No disruption changed c-di-GMP levels in the *divK*
1055 background even though some strains suppressed the motility defect while others did not. These
1056 results show a discrepancy between phenotypic effects and intracellular c-di-GMP levels.

1057

1058 **Figure 5. Artificial manipulation of c-di-GMP levels do not significantly affect phenotypes**
1059 **in the *divK* mutant.** A) Swarm expansion (dark bars) and surface adhesion (light bars) of strains
1060 that have altered c-di-GMP levels caused by expression of non-native enzymes in the wild-type
1061 and *divK* background. Constructs including the *E. coli* diguanylate cyclase *ydeH* expressed from
1062 a medium copy plasmid (med DGC) and a low copy plasmid (low DGC), the *P. aeruginosa*
1063 phosphodiesterase *pchP* (PDE) as well as a catalytically inactive variant (inactive PDE). Bars
1064 below the x-axis outline inducer used for plasmids in each strain. In the wild-type background
1065 the medium copy DGC increased motility and decreased adhesion, which is opposite the
1066 expected outcome, while the PDE reduced motility and severely reduced adhesion. In the *divK*
1067 background, no expression construct significantly altered the phenotypes. * indicates both
1068 motility and adhesion were statistically insignificant from the control strain ($p > 0.05$). B) C-di-
1069 GMP levels were measured using mass spectrometry then normalized to the amount of biomass
1070 from each sample. In the wild-type background the medium copy DGC significantly increased
1071 c-di-GMP levels while the PDE reduced c-di-GMP levels. In the *divK* background, both DGC
1072 constructs increased c-di-GMP levels, though PDE expression has no effect, despite the fact that
1073 neither DGC construct has an effect on motility and adhesion phenotypes.

1074

1075 **Figure 6. Disruption of *pleD* does not alter *pleC* or *divK* motility or adhesion, but does alter**
1076 ***divJ* motility and adhesion.**

1077 Wild-type, *pleD*, *divJ*, *divJpleD*, *divK*, *divKpleD*, *pleC*, and *pleCpleD* *B. subvibrioides* strains
1078 were analyzed for swarm expansion (A) and adhesion (B) defects using a soft agar swarm assay
1079 and a short-term adhesion assay respectively. Mutant strains were normalized to wild-type
1080 results for both assays. The *pleD* mutation has no effect on the adhesion or motility of the *pleC*
1081 or *divK* strains, but does reduce adhesion and increase motility of the *divJ* strain. In A), the bar
1082 with an asterisk indicates *divJ pleD::pCR* has statistically significant more swarm expansion than
1083 *divJ* ($p < 0.05$). In B), results with the same number of asterisks are not statistically significant
1084 from each other, but are statistically significant from results with a different number of asterisks
1085 ($p < 0.05$).

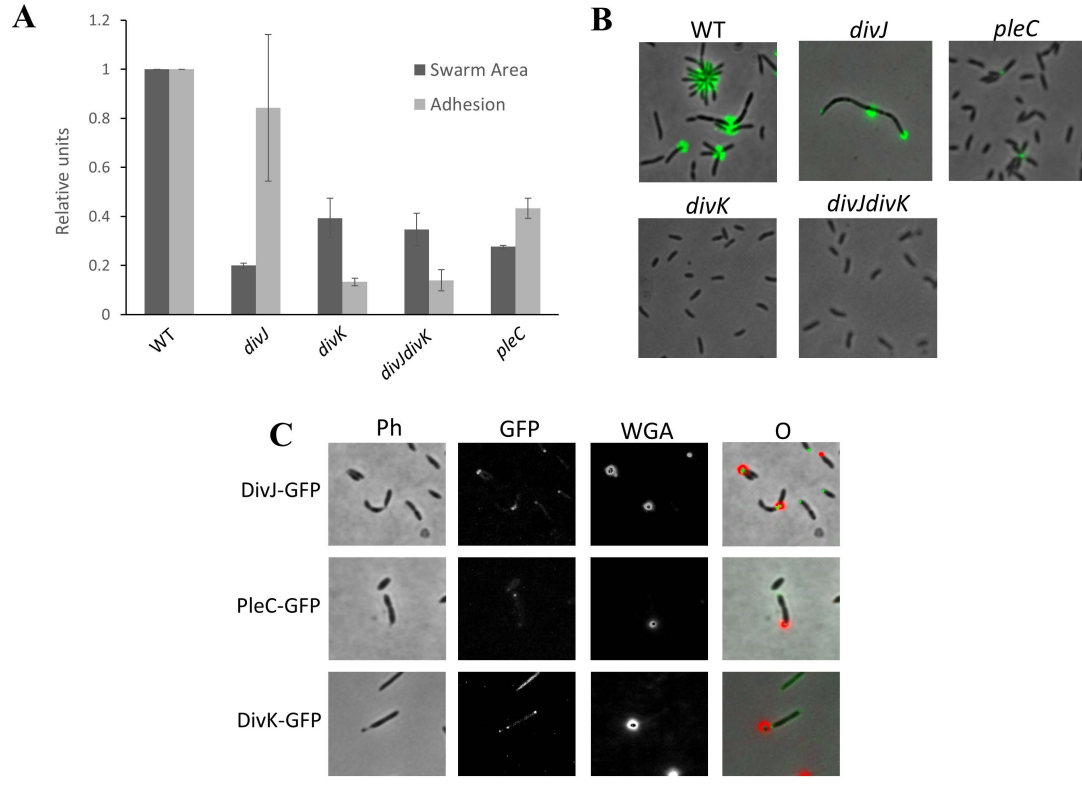
1086

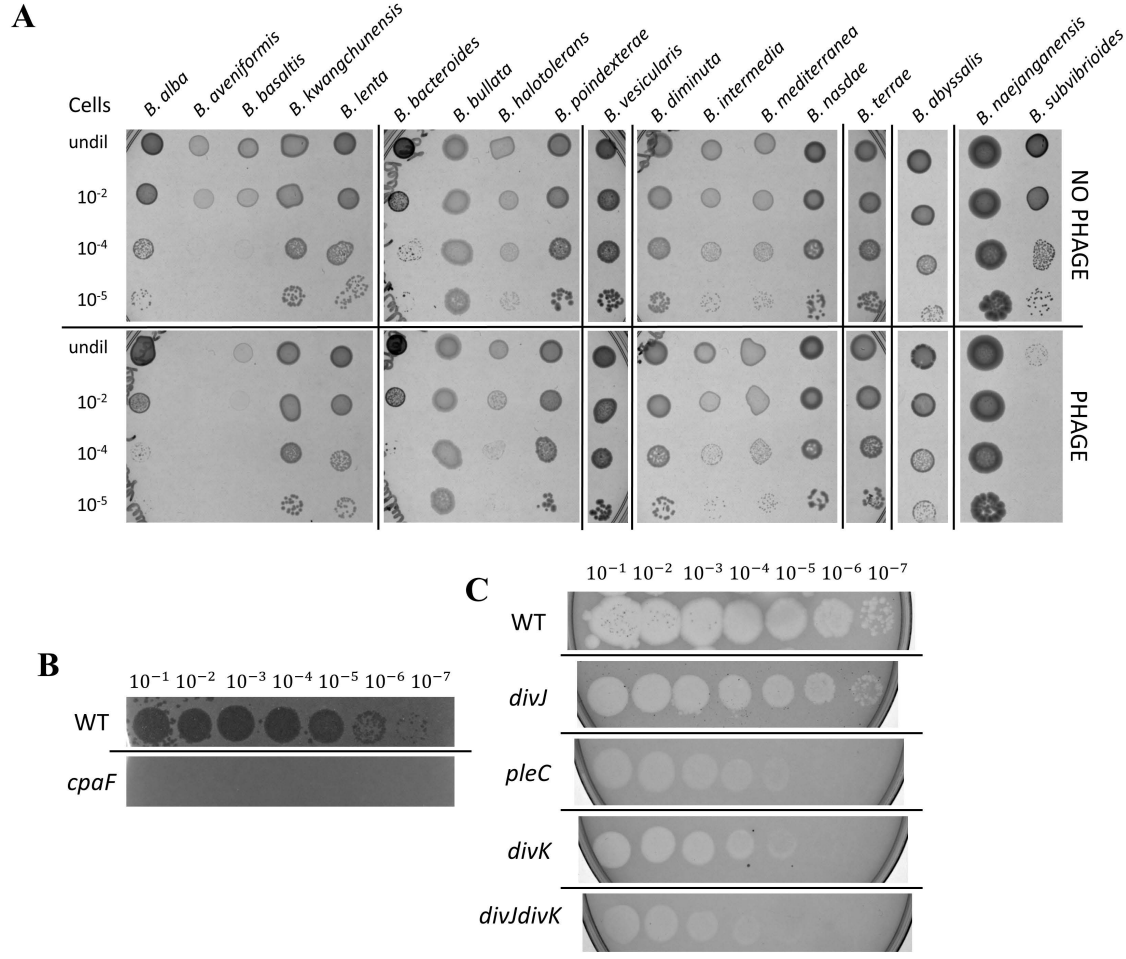
1087 **Figure 7. Disruption of *pleD* does not alter *pleC* or *divK* holdfast production or phage**
1088 **sensitivity, but does alter *divJ* holdfast production.**

1089 A) Lectin staining of holdfast material of wild-type, *pleD*, *divJ*, *divJpleD*, *divK*, *divKpleD*, *pleC*,
1090 and *pleCpleD* *B. subvibrioides* strains. The wild-type and *divJ* strains have easily detectable
1091 holdfast material. The *pleC* and *pleC pleD* strains have greatly reduced but still detectable
1092 holdfast material, while all remaining strains have no detectable holdfast. This includes the *divJ*
1093 *pleD* strain, which still displays obvious cell filamentation despite no longer producing holdfast.

1094 B) *B. subvibrioides* wild-type, *pleD*, *divJ*, *divJpleD*, *divK*, *divKpleD*, *pleC*, and *pleCpleD* strains
1095 were tested with phage Delta in soft agar phage assays. While the *pleD* disruption alters the
1096 adhesion and holdfast phenotypes of the *divJ* strain, this mutation does not alter the phage

- 1097 sensitivity of the parent, as both *divJ* and *divJpleD* strains have similar sensitivities to the phage
1098 as wild-type





Caulobacter crescentus CB15 QIFPAPTAEKGYALARAADPQLIFVEHGSSGVDGLAFTRKLRSSDLTCRE
Caulobacter henricii QIFSAPTIEKGYAMARTVDPQLIFVEHGSSGVDGLLSRKIRRSSDLVCRE
Caulobacter K31 QIFAAPSI EAGWAMARTTDPMLIFVEHASAGCDGLALARKIRRSSDLACRE
Caulobacter segnis NLWAAPTDAKALVIAQSLDPQIFVEHAGPGLDGARLTRAIRRSEFP CRQ
Brevundimonas abyssalis VVHRGEGRAALDVCREFEPTLIFTEYKGP NLDGEAFAKAVRRSNLVCRK
Brevundimonas denitrificans VVHRGEGRAALDVCREFEPTLIFTEYKGP NLDGEAFAKAVRRSNLVCRK
Brevundimonas subvibrioides EVVTESDENRVMDHAREMEPGLIFTE RSGARLDGEQLARRIRRSNLACRR
Brevundimonas bacteroides EVVTEDEGRALDHARELEPGVIFTE RSGRLDGEQFARRVRRSNMACRR
Brevundimonas diminuta EIVVEGDEARVLDLAREMEPGLICTERAGPKLDGEALVRRIRRSSLSRR
Brevundimonas naejangensis EIVVEGDEARVLDLAREMEPALIFTE RTGPKLDGEALARRIRRSSLSRR
Brevundimonas nasdae EVYSEGDEERALELLRDVEPGVIFTE RSGDRLNGETLARRIRRSSMSCRR
Brevundimonas vesicularis EVYSEGDEERALELLRDVEPGVIFTE RAGDKLNGETLARRIRRSSMSCRR
Brevundimonasa veniformis EIIIEADEKEALAAVRDFEPTLMFVERSGPRFDGETLVSKLRRSRMDARR
Brevundimonas subvibrioides DivK QTFTQREGLOAMALARQYMPDLILMDIQLPEISGLEVTKWLK-DDEELAH
: * :: : .* . :: .

